

## SUPPLEMENTARY MATERIAL

De Tobel J, Bauwens J, Parmentier G, Franco A, Pauwels N, Verstraete K, Thevissen P. The use of magnetic resonance imaging in forensic age estimation of living children and young adults systematically reviewed. *Ped Radiol*.2020. <http://dx.doi.org/10.1007/s00247-020-04709-x>

Corresponding author: Jannick De Tobel<sup>1,2,3</sup> jannick.detobel@ugent.be

1. Diagnostic Sciences – Radiology, Ghent University, Belgium
2. Imaging and Pathology – Forensic Odontology, KU Leuven, Belgium
3. Oral Diseases and Maxillofacial Surgery, Maastricht UMC+, The Netherlands

## Content

Materials and methods.....	2
Search strings .....	2
Results .....	3
Selection of studies and data .....	3
Characteristics and quality of included studies .....	4
Study characteristics .....	4
Magnetic resonance imaging approaches .....	4
Staging techniques and statistical processing .....	9
Risk of bias assessment .....	10
Quantitative synthesis .....	13
Age distributions in relation to development .....	13
Reproducibility of staging.....	28
Supplementary text references .....	31

## Materials and methods

### Search strings

In MEDLINE, the following search string was used:

1. "age determination by teeth"[MeSH Terms] OR "age determination by skeleton"[MeSH Terms] OR "determine age"[TIAB] OR "age determination"[TIAB] OR "determined age"[TIAB] OR "determining age"[TIAB] OR "estimate age"[TIAB] OR "age estimation"[TIAB] OR "estimated age"[TIAB] OR "estimating age"[TIAB] OR "assess age"[TIAB] OR "age assessment"[TIAB] OR "assessed age"[TIAB] OR "assessing age"[TIAB] OR "measure age"[TIAB] OR "age measurement"[TIAB] OR "measured age"[TIAB] OR "measuring age" [TIAB]
2. "magnetic resonance imaging"[MeSH Terms] OR "MRI"[TIAB] OR "NMR imaging"[TIAB] OR "magnetic resonance imaging"[TIAB] OR "MR imaging"[TIAB] OR "nuclear magnetic resonance imaging"[TIAB] OR "imaging, magnetization transfer"[TIAB] OR "magnetization transfer imaging"[TIAB]
3. 1-2 AND

In Embase, the following search string was used:

1. 'dental age estimation'/exp OR 'bone age determination'/exp OR 'determine age':ti,ab OR 'age determination':ti,ab OR 'determined age':ti,ab OR 'determining age':ti,ab OR 'estimate age':ti,ab OR 'age estimation':ti,ab OR 'estimated age':ti,ab OR 'estimating age':ti,ab OR 'assess age':ti,ab OR 'age assessment':ti,ab OR 'assessed age':ti,ab OR 'assessing age':ti,ab OR 'measure age':ti,ab OR 'age measurement':ti,ab OR 'measured age':ti,ab OR 'measuring age':ti,ab
2. 'nuclear magnetic resonance imaging'/exp OR 'mri':ti,ab OR 'nmr imaging':ti,ab OR 'magnetic resonance imaging':ti,ab OR 'mr imaging':ti,ab OR 'nuclear magnetic resonance imaging':ti,ab OR 'imaging, magnetization transfer':ti,ab OR 'magnetization transfer imaging':ti,ab
3. 1-2 AND

In Web of Science, the following search string was used:

1. TS=(“determine age” OR “age determination” OR “determined age” OR “determining age” OR “estimate age” OR “age estimation” OR “estimated age” OR “estimating age” OR “assess age” OR “age assessment” OR “assessed age” OR “assessing age” OR “measure age” OR “age measurement” OR “measured age” OR “measuring age”)
2. TS=(“magnetic resonance imaging” OR “MRI” OR “MR imaging” OR “nuclear magnetic resonance imaging” OR “NMR imaging” OR “imaging, magnetization transfer” OR “magnetization transfer imaging”)
3. 1-2 AND

In study registers, the following search string was used:

"age estimation" OR "age determination" OR "age assessment"

## Results

### Selection of studies and data

The database search rendered 391 single records (Fig. 1). Searching study registers generated one relevant ongoing study: the Swedish Age Assessment Study (SAAS). However, no additional data for this review were provided. Furthermore, six additional records were identified by networking at conferences on forensic science and imaging.

Early studies tended to include only descriptions of the bones' developmental changes on MRI [1]. They lacked details on age distribution within certain developmental stages. Other studies did not report sex-specific data [2-5]. Although these studies were included for qualitative synthesis, they were unsuitable for data extraction.

Moreover, 23 studies did not report the statistics on age distribution that were needed for quantitative synthesis [1-20]. When the study design indicated that such data should be available, the authors were contacted. Out of 32 authors that were contacted, only 13 responded, with ten of them

providing the requested data or statistics [19, 21-29]. This led to 33 studies suitable to create the overview graphs of development per anatomical structure in Fig. 5 of the Supplementary Material.

## Characteristics and quality of included studies

### Study characteristics

#### Magnetic resonance imaging approaches

Table 5 displays the characteristics of the MRI approaches. Most protocols used surface coils or dedicated extremity coils. A head/neck coil was used at an alternative site by two groups: to study the hand/wrist [13, 19, 25, 30], and to study the clavicles [13]. Positioning was often not reported in retrospective studies. By contrast, it proved to be a major issue in the study of clavicles, since the prone position reduced motion artefacts [14, 31]. In an attempt to avoid motion artefacts in other structures, specific fixation was applied by a bite bar [32], and stabilization was applied by vacuum pillows [19, 31].

**Table 5** Magnetic resonance imaging (MRI) characteristics of eligible studies. Studies are grouped per anatomical site and ordered per staging technique (see Table 6).

Anatomical structure	Reference	Year	MRI scanner	Coil	Positioning	MR sequence	Voxel size (mm <sup>3</sup> )	Acquisition time
Spheno-occipital synchondrosis	Ekizoglu	2016a	1.5T Siemens	NA	NA	in text T1 SE; figure captions say T2	ST 2-4 mm	NA
Molars	Baumann	2015	3T Siemens	8-channel multifunctional coil	Supine	T1 3D TSE; 3D CISS	0.6 × 0.6 × 1.0	9:47 and 8:57
Lower left third molar	Guo	2015	3T Philips	16-channel surface head/neck coil	Supine	T2 TSE	M 0.50 × 0.65 × 2.0, R 0.19 × 0.19 × 2.0	5:36
Third molars	De Tobel	2017b	3T Siemens	4-channel flexible surface head coil	Supine	T2 FSE	0.33 × 0.33 × 2.0	S 6:33; A 6:49; C 6:29
Third molars	De Tobel	2017c	3T Siemens	4-channel flexible surface head coil	Supine	T2 FSE	0.33 × 0.33 × 2.0	S 6:33; A 6:49; C 6:29
Clavicle	Hillewig	2013	3T Siemens	Loop-shaped surface coil with 11 cm bore	Prone on vacuum pillow	T1 GE VIBE	0.7 × 0.7 × 0.9	4:02
Clavicle	Tangmose	2014	1T Siemens	Surface coil	Supine; prone	T2 3D GE	0.7 × 0.7 × 1.5	6:04
Clavicle	Vieth	2014	3T Philips	2 elliptical loop shaped surface coils 14 cm x 17 cm	Prone	3D FFE	0.7 × 0.7 × 1.4	5:41
Clavicle	Schmidt	2017	3T Philips	Surface coil	Prone	T1 3D FFE FS	M 0.69 × 0.70 × 1.4, R 0.29 × 0.29 × 0.7	5:41
Clavicle	De Tobel	2019c	3T Siemens	Loop-shaped surface coil with 11 cm bore	Prone	T1 VIBE	0.7 × 0.7 × 0.9	4:02
Manubrium	Martínez Vera	2017	3T Siemens	Neck coil	Supine	T1 3D VIBE WE	0.9 × 0.9 × 0.9	NA
Proximal humerus	Ekizoglu	2018	1.5T Siemens	Extremity coil	NA	T1 TSE	0.5 × 0.5 × 3.5	1:44
Left distal radius	Dvorak	2007	1T or 1.5T	Wrist coil	Wrist above the head or at the side	T1 SE	≤ 0.5 × ≤ 0.5 × 3	NA
Left distal radius	George	2012	1.5T Siemens	Wrist coil	Prone both hands outstretched	T1 FSE	0.39 × 0.39 × 3	NA
Left distal radius	Bolivar	2015	1.5T Siemens	Wrist coil	Wrist above the head or at the side	T1 SE	≤ 0.5 × ≤ 0.5 × 3	NA
Left distal radius	Rashid	2015	1.5T Siemens	Surface coil	Wrist above the head or at the side	T1 FSE	0.5 × 0.5 × 3	5:48
Left distal radius	Tscholl	2016	1T or 1.5T	Wrist coil	Wrist above the head or at the side	T1 SE	≤ 0.5 × ≤ 0.5 × 3	NA
Left distal radius	Abdelbary	2018	0.31T open	8-channel hand/wrist coil	Supine hand next to body	T1 SE	ST 3 mm	< 7:00
Left distal radius	Sarkodie	2018	1.5T GE or Toshiba	Wrist coil	Wrist above the head or at the side	T1 SE	≤ 0.5 × ≤ 0.5 × 3	NA
Left distal radius	Schmidt	2015	3T Philips	2 elliptical loop shaped surface coils 14 cm x 17 cm	NA	T1 TSE	0.4 × 0.5 × 1.5	6:00
Left hand/wrist	Serin	2016	Philips, Siemens, GE, Toshiba	Extremity coils	NA	T1 SE	ST 2-5 mm	NA
Left distal radius	Timme	2017	3T Philips	16-channel surface head/neck coil	NA	T1 TSE	M 0.4 × 0.5 × 2.5, R 0.2 × 0.2 × 2.5	3:33
Left wrist	De Tobel	2019b	3T Siemens	Wrist coil	Supine hand next to body	T1 SE; T1 VIBE	0.20 × 0.20 × 2.0; 0.40 × 0.40 × 0.40	2:43; 5:57
Left hand/wrist	Tomei	2014	0.2T G-Scan open	Hand/wrist coil	NA	T1 3D SE	0.73 × 1.09 × 1.3	1:39 (twice if necessary)
Left hand/wrist	Serinelli	2015	0.2T G-Scan open	Small coil	NA	T1 3D SE	0.73 × 1.09 × 1.3	NA
Left hand/wrist	Terada	2013	0.3T Neomax open	1-channel dedicated coil	Seated	3D GE	0.39 × 0.78 × 1.56	2:44
Left hand/wrist	Terada	2014	0.3T Shin-Etsu open	1-channel dedicated coil	Seated	3D GE	0.39 × 0.78 × 1.56	2:44
Left hand/wrist	Terada	2016	0.3T Shin-Etsu open	1-channel dedicated coil	Seated	3D GE	0.39 × 0.78 × 1.57	2:44
Left hand/wrist	Urschler	2016	1.5T Siemens	Head coil	Prone with outstretched arm on vacuum bed	T1 3D VIBE; T1 SE; T2 3D GE	0.43 × 0.43 × 0.9; 0.86 × 0.86 × 2.0; 0.86 × 0.86 × 0.9	3:08 ; 1:00 ; 2:21
Left hand/wrist	Hojreh	2018	1.5T Siemens	Head/neck coil	Prone with outstretched arm	T1 3D VIBE WE	0.4 × 0.4 × 1.5	2:26
Left hand/wrist	Urschler	2015	3T Siemens	Head/neck coil	Prone with outstretched arm	T1 3D FLASH VIBE	0.45 × 0.45 × 0.9	< 4:00

Table 5 (continued) Magnetic resonance imaging (MRI) characteristics of eligible studies.

Anatomical structure	Reference	Year	MRI scanner	Coil	Positioning	MR sequence	Voxel size (mm <sup>3</sup> )	Acquisition time
Iliac crest	Wittschieber	2014	3T Philips	8-channel SENSE cardiac coil	NA	T1 3D GE	0.49 × 0.49 × 2.2	17:47
Proximal femur	Vo	2015	1.5T GE	Surface coil anterior + spine coil posteriorly	Supine	T1 3D spoiled GE	ST 1 mm	NA
Sacrum	Bollow	1997	1.5T Philips	Body coil	Supine with elevated legs	T1 SE, T2* opposed-phase FFE, dynamic T1 opposed-phase FFE		dynamic 11:12
Sacrum	Bray	2016	1.5T Siemens	NA	NA	T1 TSE, STIR, T1 Turbo Inversion Recovery Magnitude, postcontrast T1, DWI	1.0 × 1.0 × 3-5; 2.5 × 2.5 × 8	NA
Patellofemoral joint	Kim	2014	1.5T GE	Knee coil	NA	intermediate, T1, T2, and PD; FSE	ST 3-4 mm	NA
Distal femur	Saint-Martin	2015	1.5T Philips	NA	NA	T1 TSE	NA	NA
Knee	Dedouit	2012	1.5T Philips	Extremity coil	NA	FSE PD	ST 3.5-4 mm	4:00
Knee	Ekizoglu	2016b	3T Siemens	Knee coil	NA	T2 TSE	ST 3.5 mm	2:20
Knee	Harcke	1992	0.5T HP Vista	Knee coil (> 6 years old) or head coil (< 6 years old)	NA	T1 SE, field-echo, T2 SE	NA	NA
Knee	Laor	2002	1.5T GE	Extremity coil, torso phased-array coil, or quadrature head coil	NA	intermediate, T1, or T2; SE, FSE, some with inversion recovery; 3D spoiled gradient-recalled-echo; some with gadolinium contrast	ST 3-5 mm	NA
Proximal tibia	Jopp	2010	1.5T or 3T Philips	Knee coil	NA	1.5 T T1 TSE and PD SPIR; 3T T1 TSE and STIR long TE SENSE	ST 1.5T C 3.0 mm, S 3.5 mm; 3T C 3.0 mm, S 4.0 mm	
Distal femur	Krämer	2014a	3T Siemens	15-channel knee coil	NA	T1 TSE	0.4 × 0.4 × 3.0	1:57
Proximal tibia	Krämer	2014b	3T Siemens	15-channel knee coil	NA	T1 TSE	0.4 × 0.4 × 3.0	1:57
Knee	Fan	2016	1.5T Philips or Siemens	Knee coil	NA	T1 TSE	NA	NA
Knee	Ottow	2017	3T Philips	Surface coil	NA	T1 TSE	M 0.6 × 0.77 × 3, R 0.31 × 0.31 × 3	3:51
Knee	Auf der Mauer	2018	3T Philips	8-channel knee coil	NA	T1 SENSE	0.1875 × 0.1875 × 2	NA
Knee	Vieth	2018	3T Philips	Surface coil	NA	T1 TSE; T2 TSE SPIR	M 0.6 × 0.77 × 3, R 0.31 × 0.31 × 3; M 0.6 × 0.76 × 3, R 0.31 × 0.31 × 3	3:51; 3:08
Knee	Pennock	2018	1.5T	Extremity coil	NA	T1	NA	NA
Knee	Craig	2004	1T or 1.5T GE	NA	NA	3D fat-suppressed spoiled GRASS	ST 1.0-2.0 mm	NA
Knee	Kercher	2009	1.5T or 3T	NA	NA	T1	NA	NA
Ankle	Saint-Martin	2013	1.5T Philips	Extremity coil	NA	T1 SE	ST 2-4 mm	4:00
Distal tibia	Saint-Martin	2014	1.5T Philips	Extremity coil	NA	T1 SE	ST 2-4 mm	4:00
Ankle	Ekizoglu	2015	1.5T Siemens	Extremity coil	NA	T1 SE	0.5 × 0.5 × 3.5 mm	4:00
MFA	Stern	2017	3T Siemens	T 8-channel multifunctional coil and CW head/neck coil	TC Supine and W prone with outstretched arm	T PD TSE; CW T1 3D GE	T 0.59 × 0.59 × 1.0; C 0.9 × 0.9 × 0.9; W 0.45 × 0.45 × 0.9	NA

A = axial; C (voxel size) = clavicle; C (acquisition time) = coronal; GE (scanner) = General Electric; M = measured; MFA = multi-factorial age estimation; NA = not applicable or not reported; R = reconstructed; S = sagittal; ST = slice thickness; T = teeth; W = wrist.

Sequences: DWI = diffusion-weighted imaging, FLASH = fast low angle shot, FFE = fast field echo; FS = fat saturation; FSE = fast spin echo; GE = gradient echo; PD = proton-density-weighted; SE = spin echo; SENSE = sensitivity encoding; SPIR = spectral-presaturation-with-inversion-recovery; STIR = short-tau-inversion-recovery; T1 = T1-weighted; T2 = T2-weighted; TSE = turbo spin echo; VIBE = volume-interpolated breath-hold examination; WE = water excitation.

**Table 6** Characteristics of analyses in eligible studies. Studies are grouped per anatomical site and ordered per staging technique.

Anatomical structure	Reference	Year	Staging technique	Number of stages	Statistical analysis	Number of observers	Professional background
Spheno-occipital synchondrosis	Ekizoglu	2016a	Bassed	5	Simple linear regression	2	Radiologist and forensic pathologist
Molars (mineralization)	Baumann	2015	Demirjian	8	Descriptive	2	Dentists
Molars (eruption)	Baumann	2015	Olze	4			
Lower left third molar	Guo	2015	Demirjian	8	Descriptive	1	Dentists
Third molars	De Tobel	2017b	Demirjian	8	Descriptive	2	Medical doctor/dentistry student and researcher at radiology
Third molars	De Tobel	2017b	Köhler	10			
Third molars	De Tobel	2017c	De Tobel	8	Bayesian	2	Resident OMFS and dentist
Clavicle	Hillewig	2013	Kreitner (cfr. Schmeling 1, 2, 3, 4/5)	4	Bayesian	4	Radiologists and PhD-student
Clavicle	Tangmose	2014	Kreitner (cfr. Schmeling 1, 2, 3, 4/5)	4	Descriptive	3	MD, radiologist, forensic anthropologist
Clavicle	Vieth	2014	Schmeling and Kellinghaus	9	Descriptive	2	NA
Clavicle	Schmidt	2017	Schmeling and Kellinghaus	9	Descriptive	2	NA
Clavicle	De Tobel	2019c	Kellinghaus and Wittschieber, discarding stages 1 and 4/5, discarding substages of stage 2 (2, 3aa, 3ab, 3ac, 3b, 3c)	11, reduced to 6 in the model	Bayesian	2	Radiologist, resident OMFS, forensic anthropologists
Manubrium	Martínez Vera	2017	No staging, measurements and shape variations; semi-automatic segmentation	NA	Principal component analysis and multiple linear regression	NA	NA
Proximal humerus	Ekizoglu	2018	Schmeling and Kellinghaus	9	Descriptive	2	Radiologists
Left distal radius	Dvorak	2007	Dvorak	6	Descriptive	3	Radiologists and neurologist
Left distal radius	George	2012	Dvorak	6	Descriptive	3	Radiologists
Left distal radius	Bolivar	2015	Dvorak	6	Descriptive	3	Radiologists and sports medicine physician
Left distal radius	Rashid	2015	Dvorak	6	Descriptive	2	Radiologists
Left distal radius	Tscholl	2016	Dvorak	6	Descriptive	2	NA
Left distal radius	Abdelbary	2018	Dvorak	6	Simple linear regression, ANOVA	3	Radiologists
Left distal radius	Sarkodie	2018	Dvorak	6	Descriptive	3	Radiologists
Left distal radius	Schmidt	2015	Schmeling and Kellinghaus, including TFS	11	Descriptive	2	Forensic physician
Left hand/wrist	Serin	2016	Jopp (cfr. Schmeling 2, 3, 4/5)	3	Bayesian, transition	2	Resident and senior forensic pathologist
Left distal radius	Timme	2017	Schmeling and Kellinghaus, including TFS	11	Descriptive	2	NA
Left wrist	De Tobel	2019b	Schmeling and Kellinghaus; SE stage 4/5 substages based on VIBE stage (3c, 4, 5)	11, reduced to 8 in the model	Bayesian	2	Resident OMFS and forensic anthropologist
Left hand/wrist	Tomei	2014	Tomei	Sum of scores (range 9-85)	Simple linear regression	2	Radiologists
Left hand/wrist	Serinelli	2015	Tomei	Sum of scores (range 9-85)	Descriptive	2	NA
Left hand/wrist	Terada	2013	Tanner-Whitehouse-2-Japan RUS	Sum of scores	Simple linear regression	2	Orthopedic specialists
Left hand/wrist	Terada	2014	Tanner-Whitehouse-2-Japan RUS	Sum of scores	Simple linear regression	3	Orthopedic specialists and radiologist
Left hand/wrist	Terada	2016	Tanner-Whitehouse-2-Japan RUS	Sum of scores	Simple linear regression	2	Orthopedic specialist and radiologist
Left hand/wrist	Urschler	2016	Greulich-Pyle; Tanner-Whitehouse-2	Age categories; sum of scores	Descriptive	2	Radiologists
Left hand/wrist	Hojreh	2018	Greulich-Pyle	Age categories	Descriptive	2	Radiologists
Left hand/wrist	Urschler	2015	Continuous	Age categories	RRF	NA	NA

Table 6 (continued) Characteristics of analyses in eligible studies.

Anatomical structure	Reference	Year	Staging technique	Number of stages	Statistical analysis	Number of observers	Professional background
Iliac crest	Wittschieber	2014	Webb (cfr. Schmeling 1, 2, 3, 4)	8	Descriptive	1	NA
Proximal femur	Vo	2015	Adjusted Dvorak; angle of Nötzli	6; continuous angles	ANOVA	3	Radiologists
Sacrum SA	Bollow	1997	Bollow (cfr. Schmeling 2, 3, 4/5); ADC continuous	3	Descriptive	3	Radiologists
Sacrum LA	Bollow	1997	Bollow	3			
Sacrum SA	Bray	2016	Bollow (cfr. Schmeling 2, 3, 4/5); ADC continuous	3	ANOVA	2	Radiologists
Patellofemoral joint	Kim	2014	Open/closing or closed; measurements	2	Regression	2	Radiologists
Distal femur	Saint-Martin	2015	Fused or not	2	Regression	2	Forensic pathologists
Knee	Dedouit	2012	Dedouit	5	Transition	2	Radiologist and forensic pathologist
Knee	Ekizoglu	2016b	Dedouit	5	Descriptive	2	Radiologists
Knee	Harcke	1992	Harcke (cfr. Kellinghaus 2a/2b, 2c, 3, 4/5)	4	None	NA	NA
Knee	Laor	2002	Laor (metaphyseal stripe; cfr. Schmeling 2 with stripe, 3 with stripe, 4/5 with stripe, 4/5 no stripe)	4	Descriptive	2 consensus	Radiologists
Proximal tibia	Jopp	2010	Jopp (cfr. Schmeling 2, 3, 4/5)	3	Descriptive	2	Radiologists
Distal femur	Krämer	2014a	Schmeling and Kellinghaus	9	Descriptive	2	NA
Proximal tibia	Krämer	2014b	Schmeling and Kellinghaus	9	Descriptive	2	Radiologists
Knee	Fan	2016	Kramer (cfr. Kellinghaus 2, 3a, 3b, 3c, 4, 5)	6	Simple linear regression	2	NA
Knee	Ottow	2017	Schmeling and Kellinghaus	9	Descriptive	2	NA
Knee	Auf der Mauer	2018	Jopp (cfr. Schmeling 2, 3, 4/5) and SKJ	3	Descriptive	3	Forensic pathologist
Knee	Vieth	2018	Vieth	6	Descriptive	2	NA
Knee	Pennock	2018	Pennock	Age categories	Descriptive	2	NA
Knee	Craig	2004	Continuous	Areas at superior-inferior MIP, volumes	Simple linear regression	NA	Radiologists
Knee	Kercher	2009	Physeal volume continuous	NA	Simple linear regression	NA	NA
Ankle	Saint-Martin	2013	Jopp (cfr. Schmeling 2, 3, 4/5)	3	Bayesian, transition	2	Forensic pathologists, trained by senior radiologist
Distal tibia	Saint-Martin	2014	No staging, signal intensity 3D or 2D graph	Minor or adult	Descriptive	NA	NA
Ankle	Ekizoglu	2015	Jopp (cfr. Schmeling 2, 3, 4/5)	3	Descriptive	2	Radiologists
MFA	Stern	2017	Continuous	Ages as output	RRF and DCNN	NA	NA

ADC = apparent diffusion coefficient; ANOVA = analysis of variance; DCNN = deep convolutional neural network; LA = lateral apophyses; MFA = multi-factorial age estimation; MIP = maximum intensity projection, NA = not applicable or not reported; OMFS = oral and maxillofacial surgery; RRF = random regression forest; SA = segmental apophyses; SKJ = cumulative score of the knee joint; TFS = threefold stratification sign.

### Staging techniques and statistical processing

Table 6 displays the different staging techniques, how they were analyzed for age estimation, and who conducted the staging. In those tables, studies are grouped according to anatomical site from head to toe: skull, teeth, chest, upper limb, hip, and lower limb.

In addition to the generally applicable most elaborate staging technique for bone development (Table 2), two staging techniques should be considered MR-sequence-specific: Dedouit [33, 34] and Vieth [35]. Similarly, four MR-specific signs of bone development have been reported: the threefold stratification sign in wrist MRI [27, 36, 37], and the metaphyseal stripe [2], the oreo-sign and the crack-sign [10] in knee MRI.

In an attempt to combine information from different bones, Auf der Mauer et al. (2018) calculated the sum of the stages in three knee bones on MRI [26]. Similarly, the Tomei (MRI) [38] and Tanner-Whitehouse (radiograph) [39] hand/wrist atlas techniques calculate a sum of individual bone scores. Conversely, the Greulich-Pyle hand/wrist (radiograph) [40] and Pennock knee (MRI) [10] atlas techniques use standard images per age category instead of scores. Finally, (semi-) automatic techniques extract continuous data from the MRI to relate them to age [3, 4, 7, 9, 13, 25].

A final characteristic in relation to image analysis lies in the observers' background and experience. Table 6 of the Supplementary Material clearly demonstrates the multidisciplinary nature of age estimation. Some studies reported how many years of experience the observers had, either in their discipline (range 2 to 20 years) [5, 41], or with age estimation (range 1 to 9 years) [27, 28].

## Risk of bias assessment

**Table 7** Risk of bias assessment. References are ordered in the same way as in Tables 1 and 5-6.

Green cells indicate that the issue was addressed appropriately. Red cells indicate that the issue was addressed inappropriately. Yellow cells indicate that the issue was not reported.

Reference	Year	Selection bias					Performance bias		Attrition bias		Detection bias		Reporting bias		Other bias	
		Did the study avoid inappropriate exclusions?	Do the included patients match the review question?	Was the study population evenly distributed in age?	Did the study population show a uniform biological origin?	Did the study population show a uniform socio-economic status (SES)?	Was the index test and its conduct in agreement with the review question?	Was the interpretation of the index test in agreement with the review question?	Were incomplete outcome data adequately addressed?	Were reasons for not assessable images specified?	Were missing values equally distributed among ages?	Were the observers blinded for the age of the participants?	Were the observers blinded for the sex of the participants?	Was there no selective outcome reporting?	Was there no conflict of interest from funding?	Was there no other possible bias?
Ekizoglu	2016a	?	+	+	?	?	-	+	+	?	+	?	?	-	+	?
Baumann	2015	+	+	-	?	?	+	-	+	+	?	+	?	+	+	?
Guo	2015	+	+	+	+	?	+	-	+	+	?	?	?	+	+	?
De Tobel	2017b	+	+	+	+	+	+	-	+	+	?	+	-	+	+	?
De Tobel	2017c	+	+	+	+	+	+	+	+	+	?	+	-	+	+	?
Hillewig	2013	+	+	+	+	?	+	+	+	+	?	+	-	+	+	?
Tangmose	2014	+	+	-	-	?	+	+	+	+	-	+	?	+	?	?
Vieth	2014	+	?	+	+	?	+	+	+	+	?	+	-	+	+	-
Schmidt	2017	+	+	+	+	?	+	+	+	+	?	+	+	+	+	?
De Tobel	2019c	+	+	+	+	+	+	+	+	+	-	+	-	+	+	?
Martínez Vera	2017	+	+	+	+	?	+	+	+	+	?	+	-	+	+	?
Ekizoglu	2018	?	?	-	?	?	-	+	+	+	+	+	+	+	+	?
Dvorak	2007	?	?	-	-	?	+	+	+	-	+	+	-	+	+	-
George	2012	+	?	+	+	?	+	+	?	?	+	+	-	+	+	-
Bolivar	2015	+	?	?	?	+	+	+	+	?	+	+	-	+	+	-
Rashid	2015	+	?	+	+	?	+	+	?	?	+	?	-	-	?	-
Tscholl	2016	+	+	-	+	?	+	+	+	?	?	+	-	-	+	-
Abdelbary	2018	+	+	-	+	?	+	+	+	+	+	?	-	+	+	-
Sarkodie	2018	+	-	-	+	?	+	+	+	+	+	+	-	-	+	-
Schmidt	2015	+	?	+	+	?	+	+	+	?	+	+	-	-	+	-
Serin	2016	?	+	-	?	?	-	+	?	+	+	?	+	-	?	?
Timme	2017	+	+	+	?	?	+	+	+	?	+	+	+	-	+	?
De Tobel	2019b	+	+	+	+	+	+	+	+	?	+	+	-	+	+	?
Tomei	2014	+	+	-	+	?	+	+	+	?	+	?	+	?	+	-
Serinelli	2015	+	+	?	+	?	+	+	+	?	+	+	-	+	?	-
Terada	2013	+	+	?	+	?	+	-	+	+	?	+	?	+	?	-
Terada	2014	+	+	?	+	?	+	-	+	+	?	+	?	+	?	-
Terada	2016	+	+	?	+	?	+	-	+	+	?	+	?	+	?	-
Urschler	2016	+	-	-	+	?	+	-	+	?	?	+	-	+	+	-
Hojreh	2018	+	+	-	-	?	+	-	+	+	+	+	?	+	+	-
Urschler	2015	+	+	-	+	?	+	+	?	?	+	+	-	+	+	-

Table 7 (continued) Risk of bias assessment.

Reference	Year	Selection bias					Performance bias		Attrition bias		Detection bias		Reporting bias		Other bias	
		Did the study avoid inappropriate exclusions?	Do the included patients match the review question?	Was the study population evenly distributed in age?	Did the study population show a uniform biological origin?	Did the study population show a uniform socio-economic status (SES)?	Was the index test and its conduct in agreement with the review question?	Was the interpretation of the index test in agreement with the review question?	Were incomplete outcome data adequately addressed?	Were reasons for not assessable images specified?	Were missing values equally distributed among ages?	Were the observers blinded for the age of the participants?	Were the observers blinded for the sex of the participants?	Was there no selective outcome reporting?	Was there no conflict of interest from funding?	Was there no other possible bias?
Wittschieber	2014	+	?	+	+	?	+	+	+	+	?	+	-	+	+	-
Vo	2015	+	+	-	?	?	+	+	+	?	?	+	?	+	+	-
Bollow	1997	?	-	?	?	?	-	-	+	+	?	?	?	+	+	-
Bray	2016	?	+	-	?	?	-	-	+	+	?	?	?	+	+	-
Kim	2014	+	-	-	?	?	-	-	?	?	?	+	+	+	+	?
Saint-Martin	2015	?	+	+	?	?	-	+	?	?	?	+	-	+	?	?
Dedouit	2012	+	+	-	?	?	-	+	?	+	+	+	+	-	?	?
Ekizoglu	2016b	?	+	-	?	?	-	+	?	?	?	?	?	-	?	-
Harcke	1992	?	+	-	?	?	-	-	?	?	?	?	?	?	?	?
Laor	2002	+	-	?	?	?	-	-	+	?	+	+	+	+	?	-
Jopp	2010	+	+	-	+	+	+	+	?	+	+	+	-	-	+	-
Krämer	2014a	?	+	-	?	?	-	+	?	?	+	+	+	+	?	?
Krämer	2014b	?	+	-	?	?	-	+	?	?	+	+	+	+	?	?
Fan	2016	?	+	-	+	?	-	+	?	+	?	?	-	?	?	?
Ottow	2017	?	+	+	+	?	+	+	+	+	+	+	+	+	+	?
Auf der Mauer	2018	+	+	-	+	+	+	+	+	+	+	+	-	-	+	?
Vieth	2018	?	+	+	+	?	+	+	+	+	+	+	+	+	+	?
Pennock	2018	+	+	+	?	?	-	+	?	?	+	-	-	-	+	-
Craig	2004	?	+	-	?	?	-	-	?	?	+	?	?	+	?	-
Kercher	2009	?	+	?	?	?	-	-	+	?	?	?	?	?	?	-
Saint-Martin	2013	?	+	-	?	?	-	+	?	+	+	+	+	-	+	?
Saint-Martin	2014	?	+	-	?	?	-	+	?	+	+	+	+	+	+	?
Ekizoglu	2015	?	+	-	?	?	-	+	?	+	?	?	?	+	?	?
Stern	2017	+	+	+	+	?	+	+	?	+	+	+	-	+	+	?

Performance bias was caused by participants being scanned for a clinical indication, which was not in agreement with the review question. The second source of performance bias considered the interpretation of the images and was caused by applying a staging technique which might not be suitable for MRI [15-17, 19, 21, 22, 30, 42], or by focusing on development, rather than age estimation [1-5, 7, 8].

Attrition bias was caused by a lack of information about why data were missing [43], or by more missing values in certain age categories [14, 28, 43]. Especially in clavicle studies, motion artefacts and anatomical shape variants caused missing data, ranging from 1% [31] to 36% [28]. Molars were not assessable on MRI in 0-15% [21], the left wrist in 1% [27] to 14% [17], and a knee scan was repeated up to three times in case of motion artefacts [44].

Detection bias was a minor issue, since it can be assumed that observers were blinded for the age of participants, even when it was not reported. Blinding for sex seems less important, since in practice the sex is also known.

Reporting bias was caused as a result of neglecting to specify which observer's results were reported. Although several studies received funding from governmental agencies or sports associations, they were not considered to cause conflicts of interest.

Other sources of bias were manifold:

- not sex-specific [2-5, 7];
- a small age range of the study population (i.e. 5 years or less) [6, 12, 23, 36, 45, 46];
- a lower age limit close to 18 (i.e. less than 2 years lower than 18) [36, 45, 46];
- an upper age limit close to 18 (i.e. less than 2 years higher than 18) [3, 5, 6, 10, 20, 24, 30, 43, 47-50];
- an upper age limit younger than 18 [12, 15-19];
- age expressed in years without fractions, so that subjects who exceeded 6 months of a year would be counted as reaching the upcoming age [49];
- only birth years were recorded, no birth dates [34];
- unclear statistical approach [19].

## Quantitative synthesis

### Age distributions in relation to development

Fig. 4 explains how differences in reported data were handled to create the graphs in Fig. 5. Tables with the statistics used to create the graphs in Fig. 5 can be obtained from the corresponding author upon request.

To quantify how well the age distributions increased with increasing stages, several studies reported correlation coefficients. The Pearson correlation coefficient was reported for the manubrium (0.66-0.73) [9], and hand/wrist (0.90-0.92) [16, 18]. The Spearman correlation coefficient was reported for the spheno-occipital synchondrosis (0.73-0.86) [51], clavicle (-0.043-0.77) [14, 52], proximal humerus (0.63-0.65) [41], distal radius (0.07-0.77) [6, 12], hand/wrist (0.94-0.96) [50], proximal femur (0.79-0.83) [20], distal femur (0.76-0.85) [26, 34], proximal tibia (0.76-0.85) [26, 34], proximal fibula (0.77) [26], and knee (0.80-0.98) [10, 26]. Remarkably, the correlation coefficients were mostly higher in males than in females.

Furthermore, two studies applied transition analysis and reported mean ages of transition from one stage to another [33, 53]. They only applied main stages, without substaging.

**Fig. 4** Clarification of what the box-plots in Fig. 5 indicate.

When the first choice statistics were not available, the second choice statistics were used to create the graph instead. When the second choice statistics were not available, the third choice statistics were used. This needs to be taken into account when interpreting the graphs.

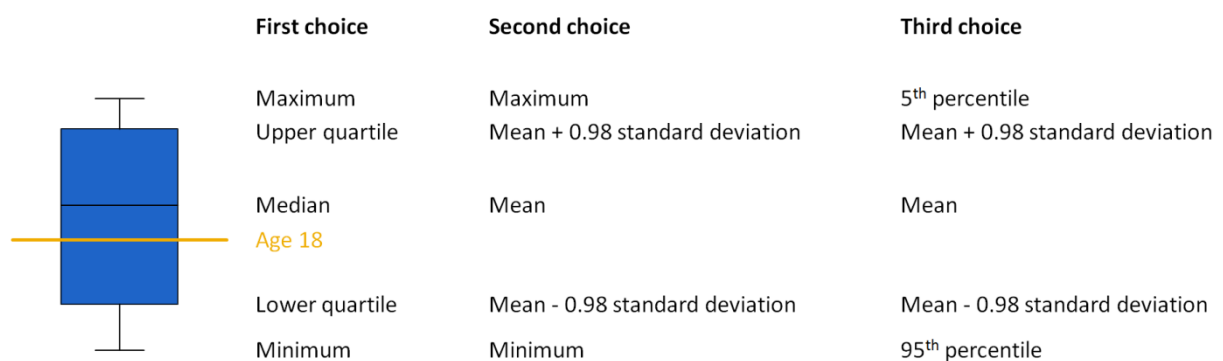


**Fig. 5** Sex-specific age distributions per developmental stage of different anatomical structures. Similar staging techniques for development are grouped. Main stages are jointly indicated on top of the graph. Note that stages were re-named according to the most elaborate staging technique (Table 2), if appropriate. Below the main stages, the number of participants per boxplot is indicated. Age is displayed on the ordinate, uniformly calibrated for all graphs. References and stages are included on the abscissa. If results from different observers were reported, those are separately included in the graph. Per graph, results from the same study are indicated by the same color of the box-plots.

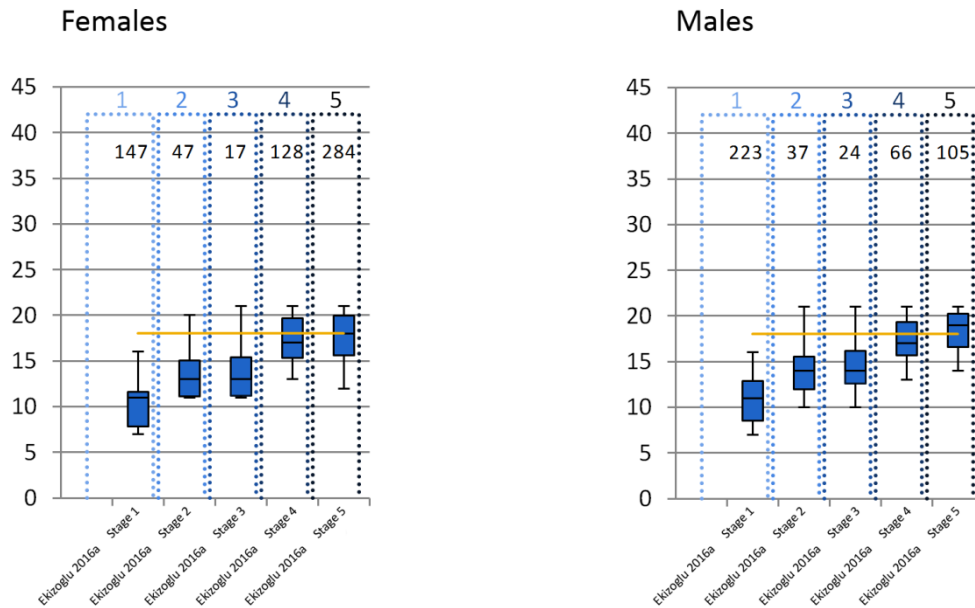


**Fig. 5a** Speno-occipital synchodrosis – Based staging technique.

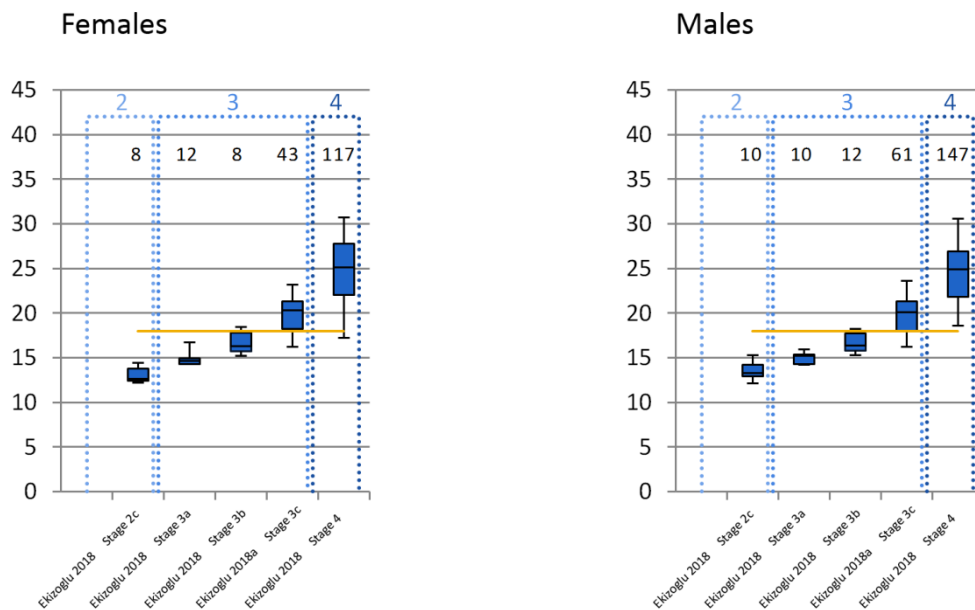
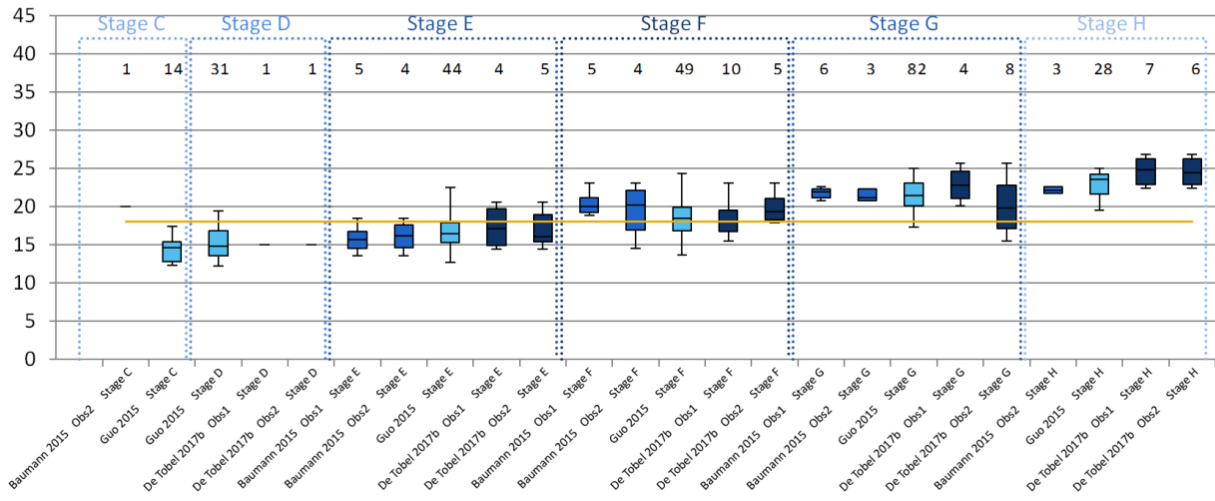


**Fig. 5b** Proximal humerus – Most elaborate staging technique.

### Females



### Males

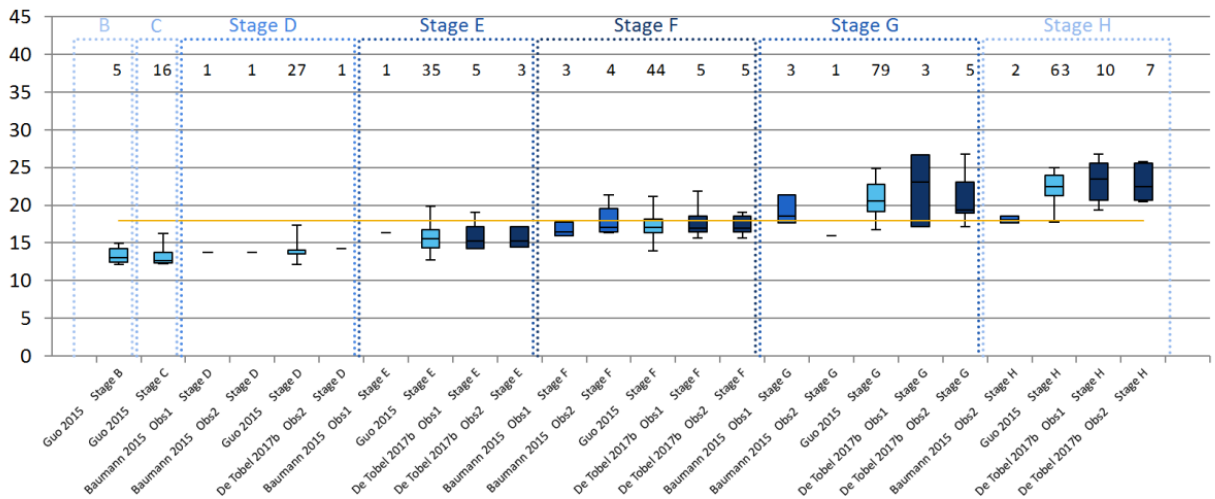


Fig. 5c Lower left third molar – Demirjian staging technique.

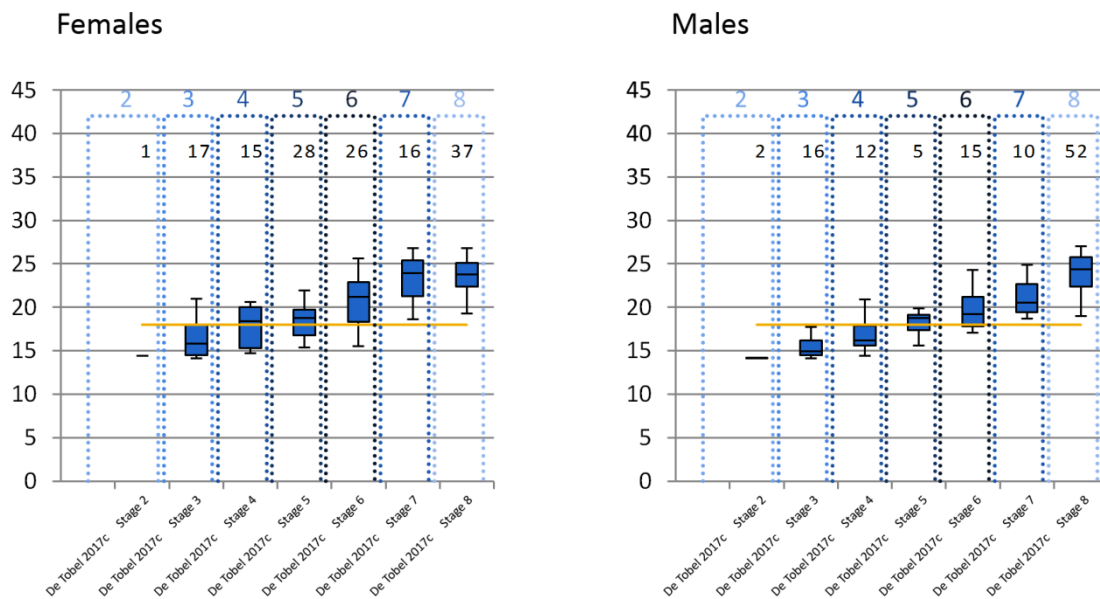
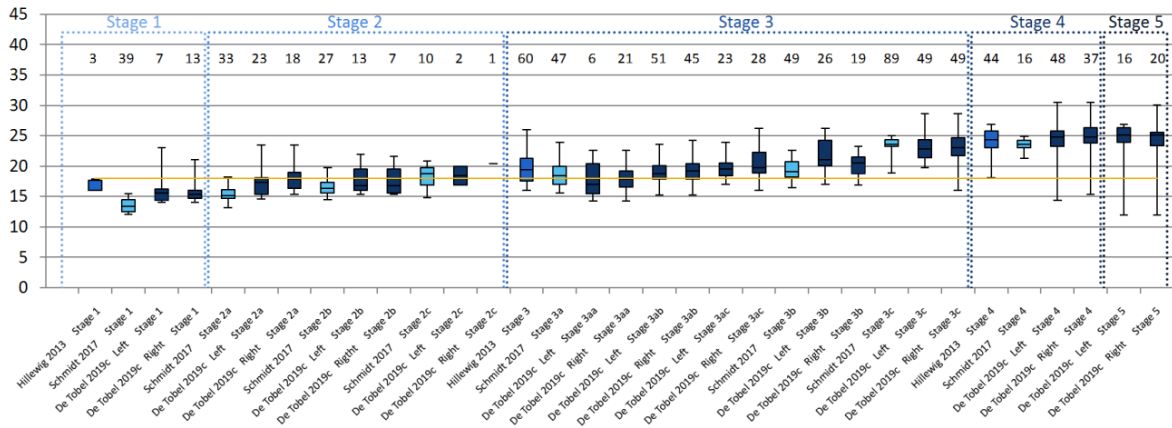
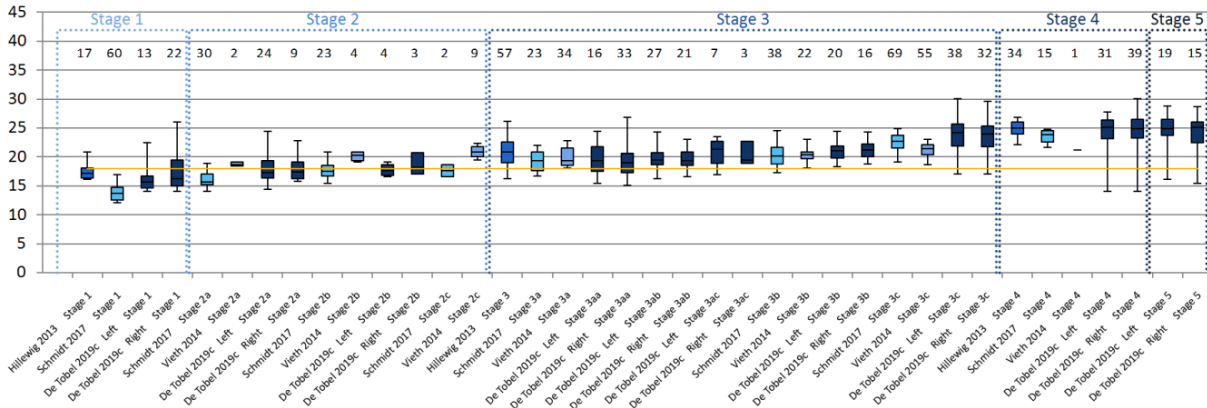


Fig. 5d Lower left third molar – De Tobel staging technique.

### Females



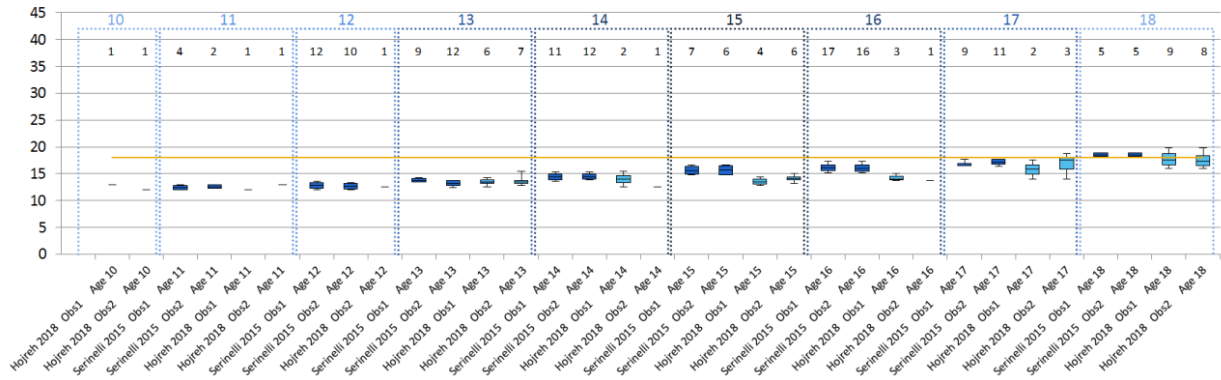
### Males



**Fig. 5e** Sternal end of the clavicles – Most elaborate staging technique.

When both clavicles were reported separately, they are separately included in the graph.

## Females



## Males

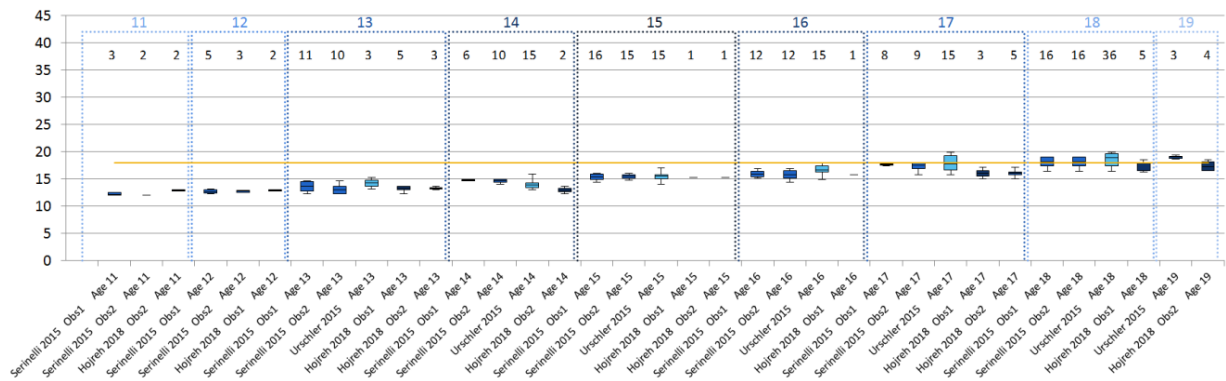
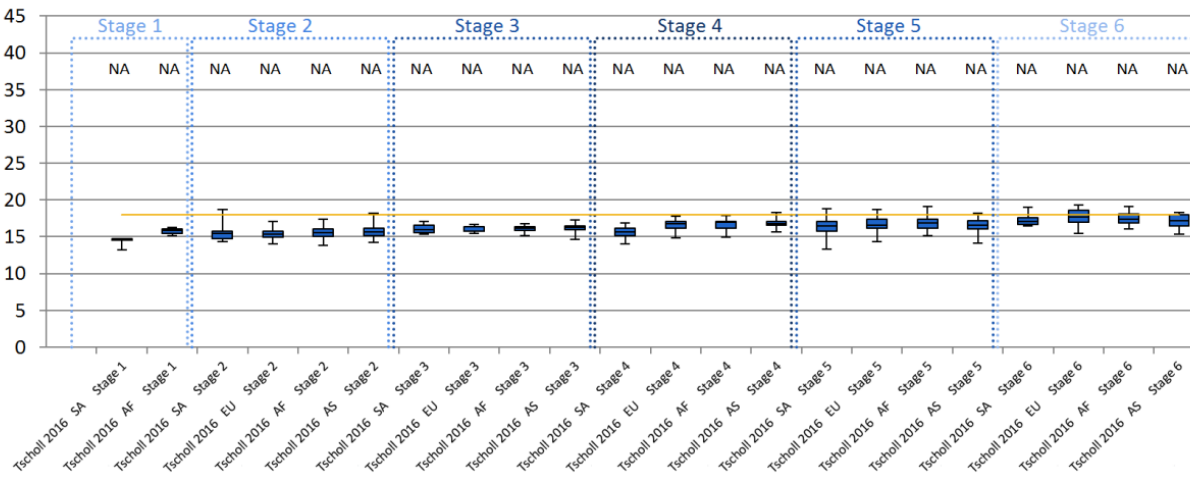


**Fig. 5f** Left hand/wrist spin echo (Serinelli et al. 2015) and VIBE (Urschler et al. 2015 and Hojreh et al. 2018) sequence – Atlas and automated technique.

Note that Serinelli et al. 2015 applied the MRI-specific atlas, Hojreh et al. 2018 applied the Greulich-Pyle atlas, and Urschler et al. 2015 applied an automated method.

### Females



### Males

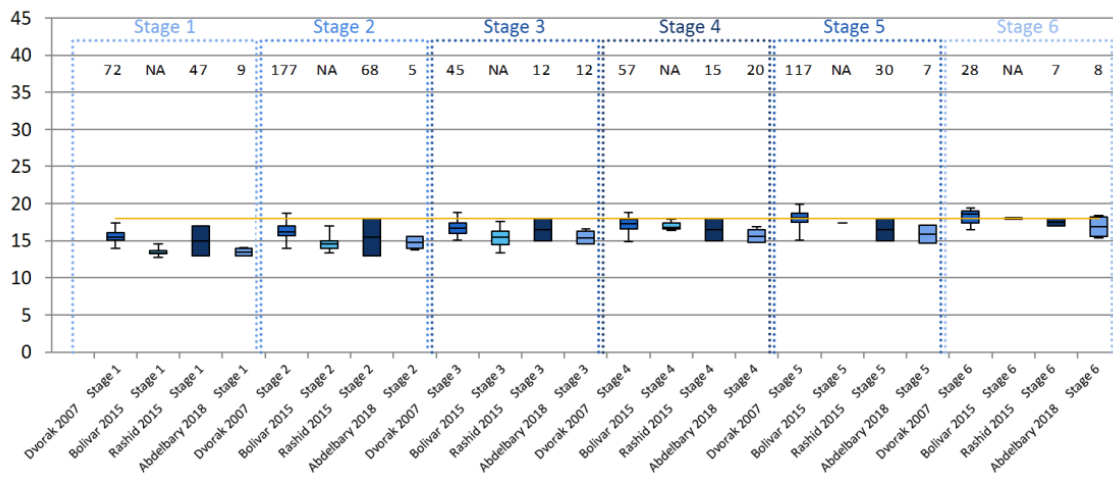
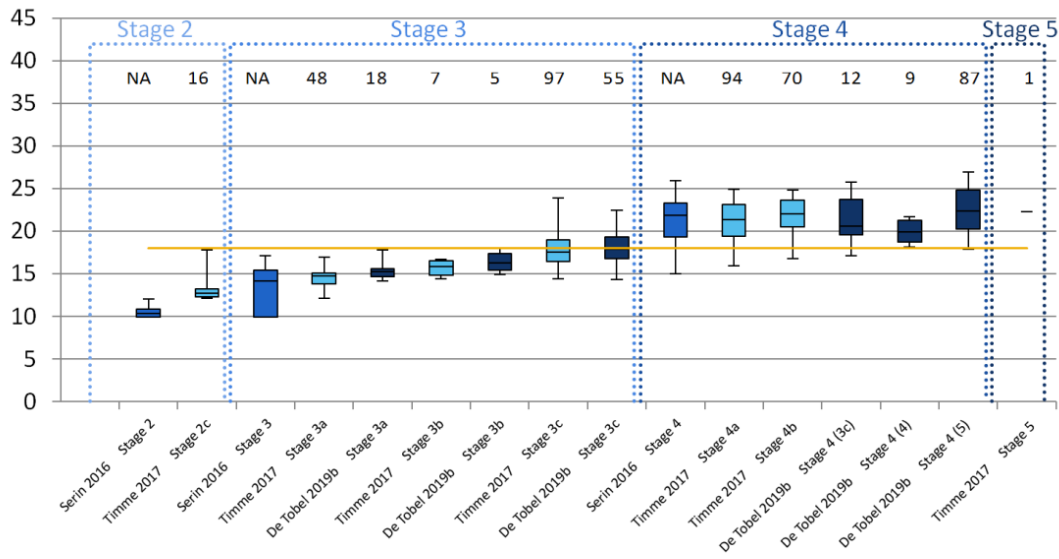


**Fig. 5g** Left distal radius spin echo sequence – Dvorak staging technique.

SA = Latin American; AF = African; EU = European; AS = Asian.

### Females



### Males

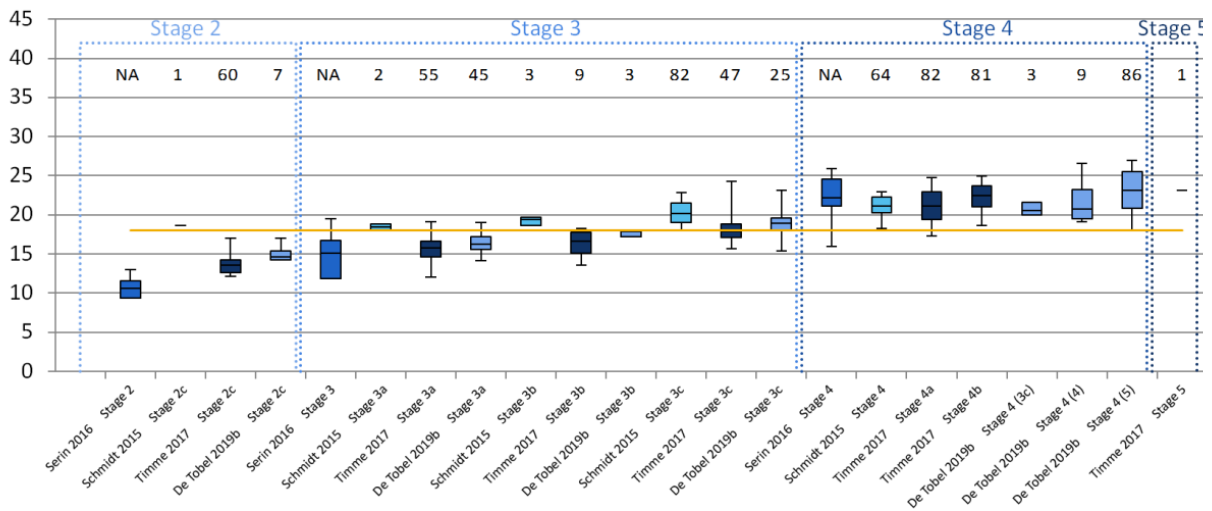


**Fig. 5h** Left distal radius spin echo sequence – Most elaborate staging technique.

For De Tobel et al. 2019, the stages between brackets correspond with added VIBE information.

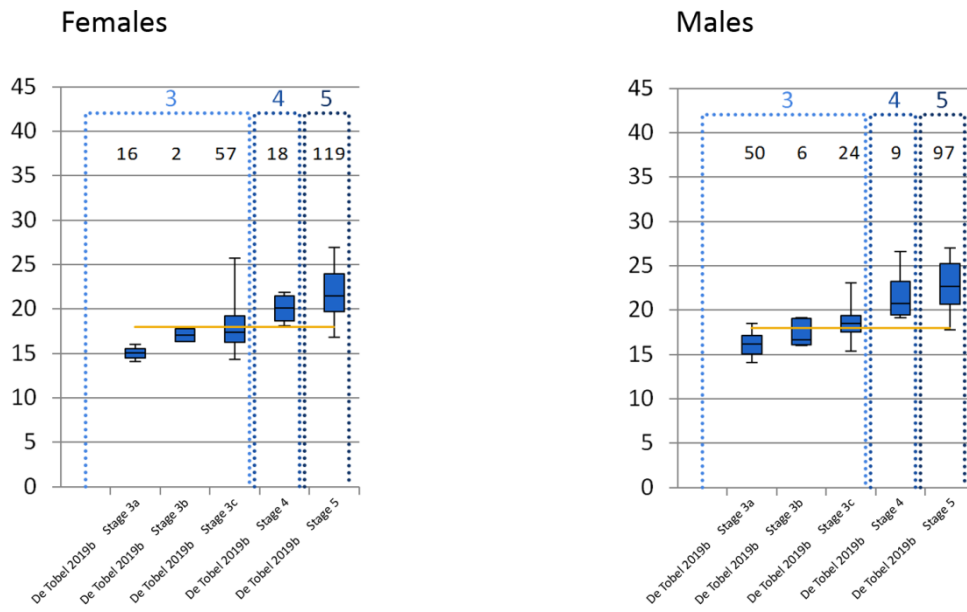
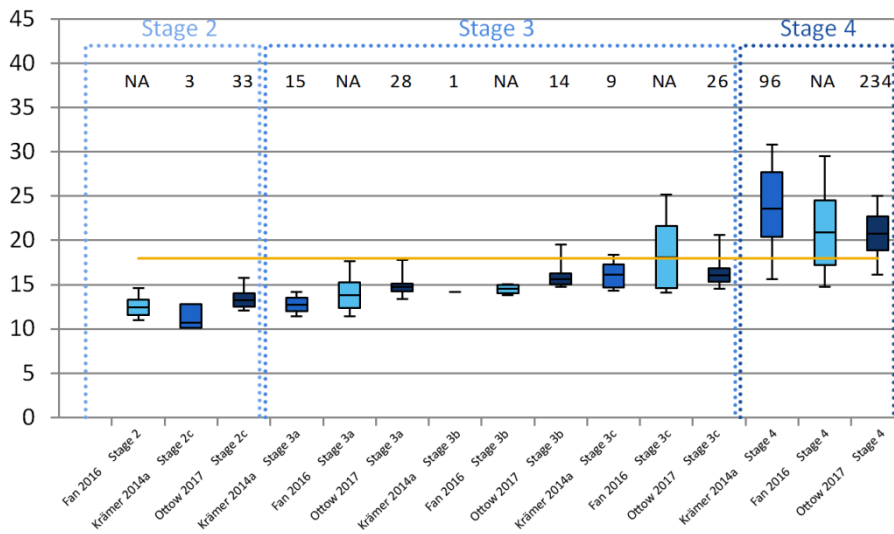


Fig. 5i Left distal radius VIBE sequence – Most elaborate staging technique.

Females



Males

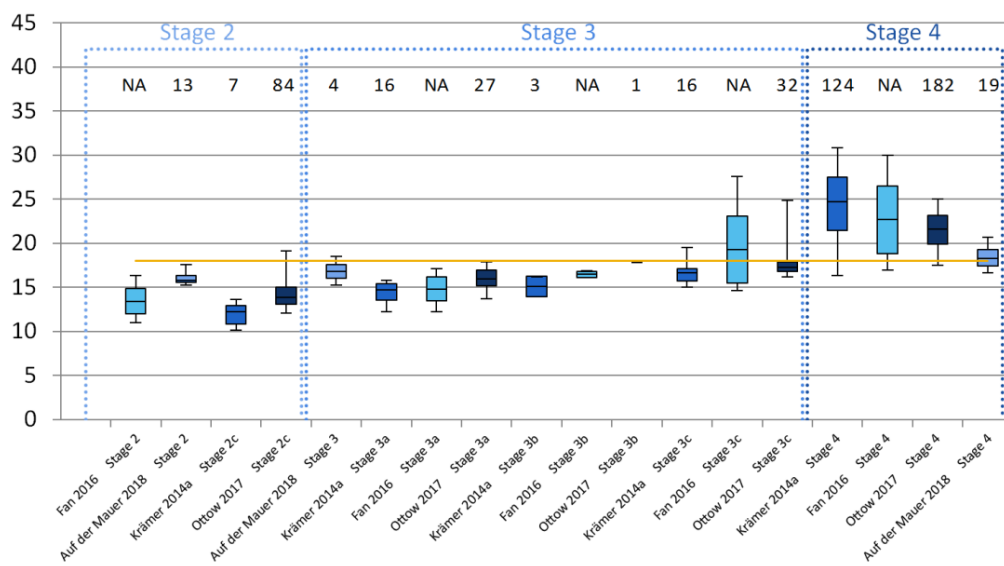
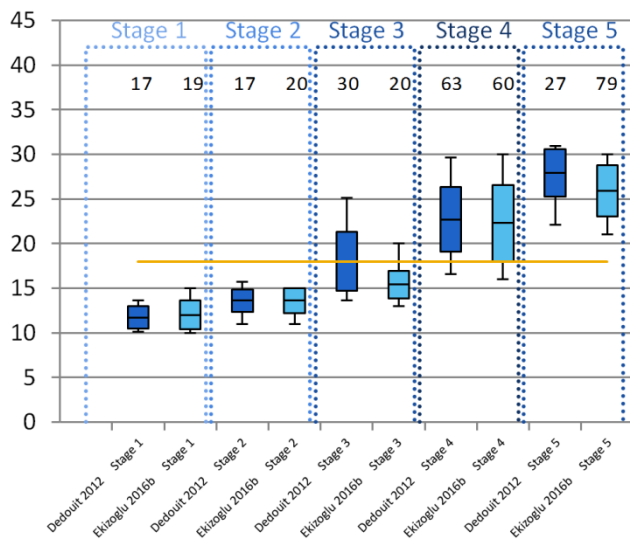


Fig. 5j Distal femur – Most elaborate staging technique.

### Females



### Males

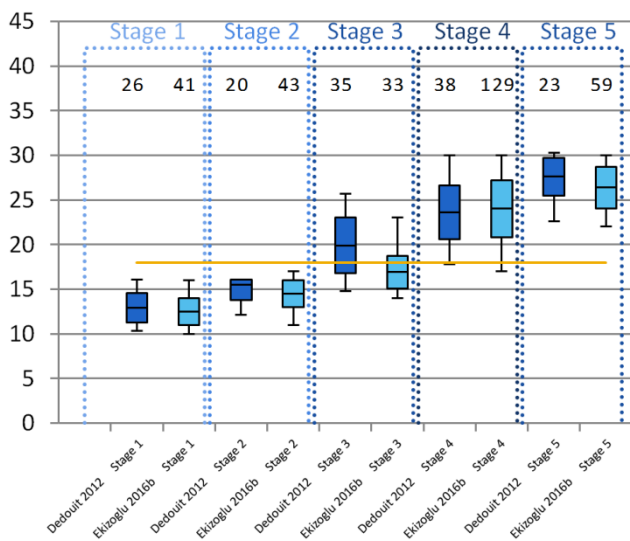
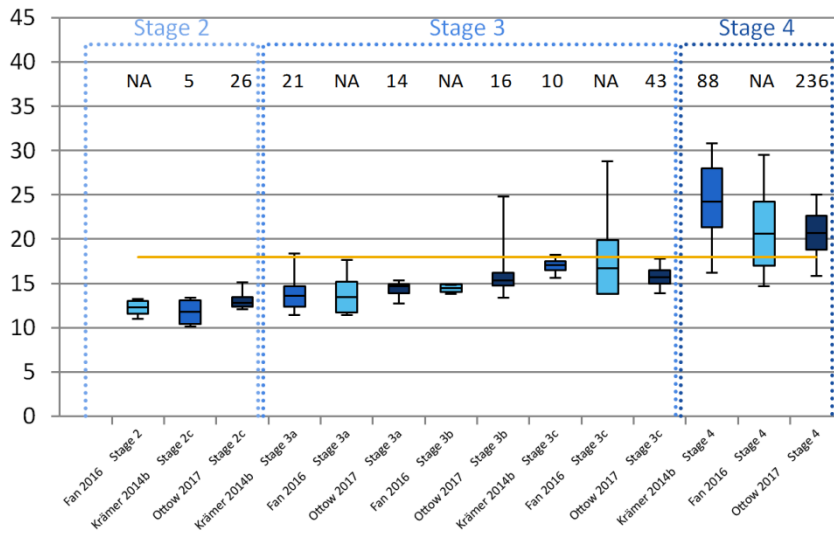


Fig. 5k Distal femur – Dedouit staging technique.

Females



Males

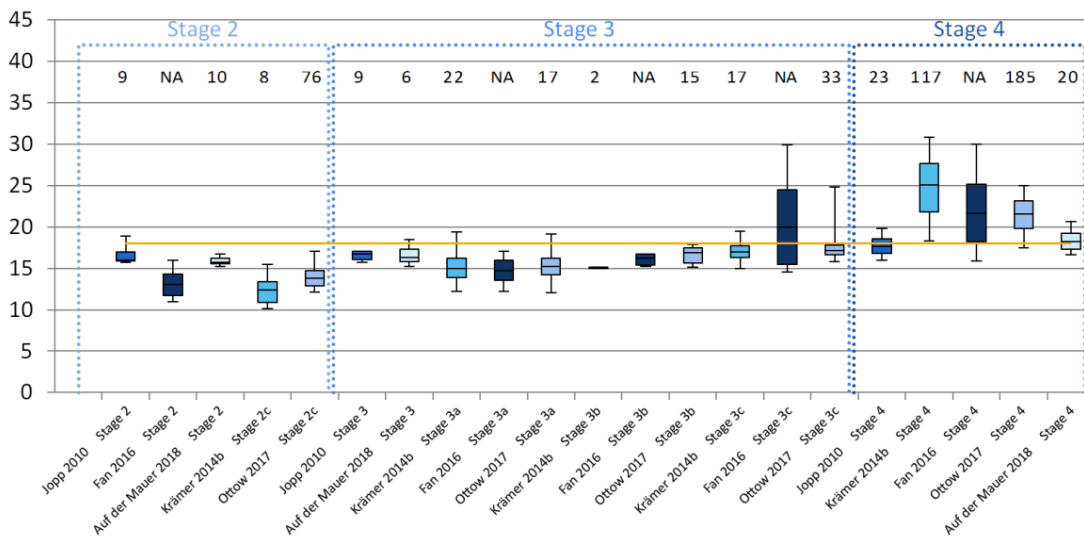
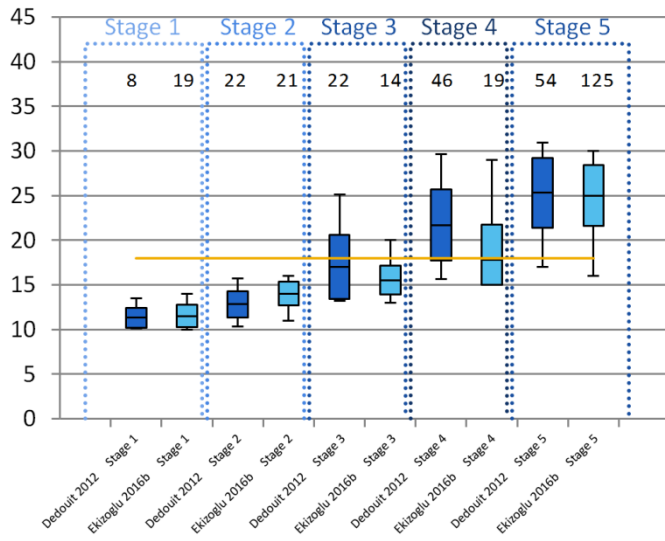


Fig. 51 Proximal tibia – Most elaborate staging technique.

### Females



### Males

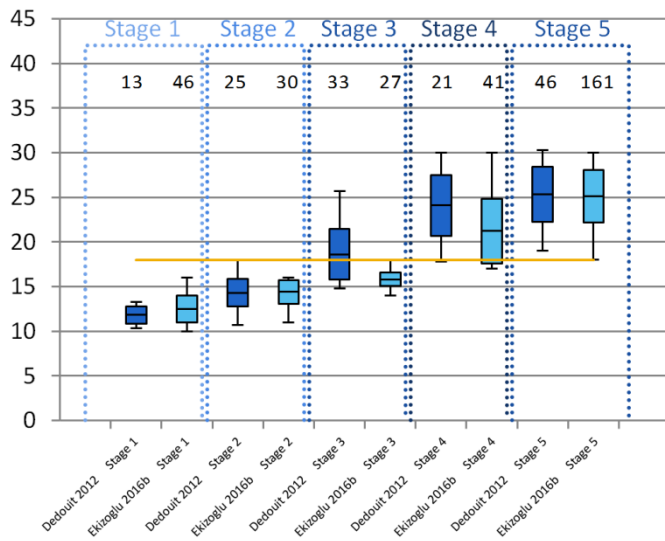


Fig. 5m Proximal tibia – Dedouit staging technique.

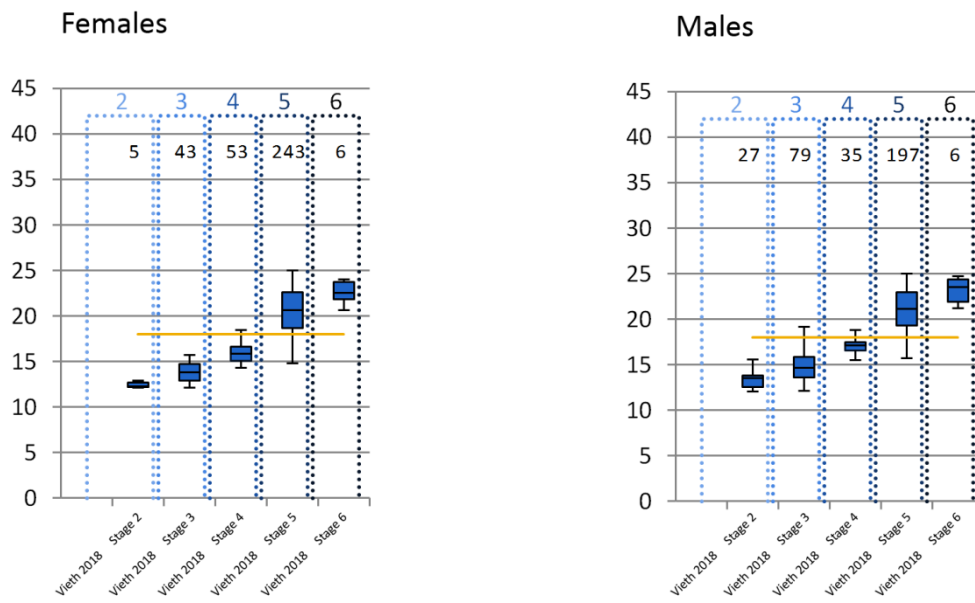


Fig. 5n Distal femur – Vieth staging technique.

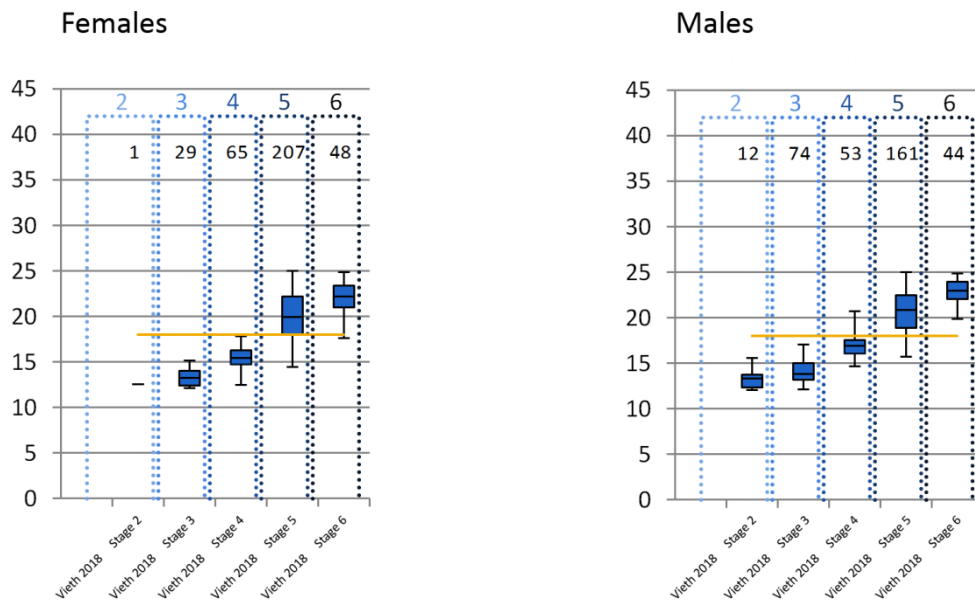


Fig. 5o Proximal tibia – Vieth staging technique.

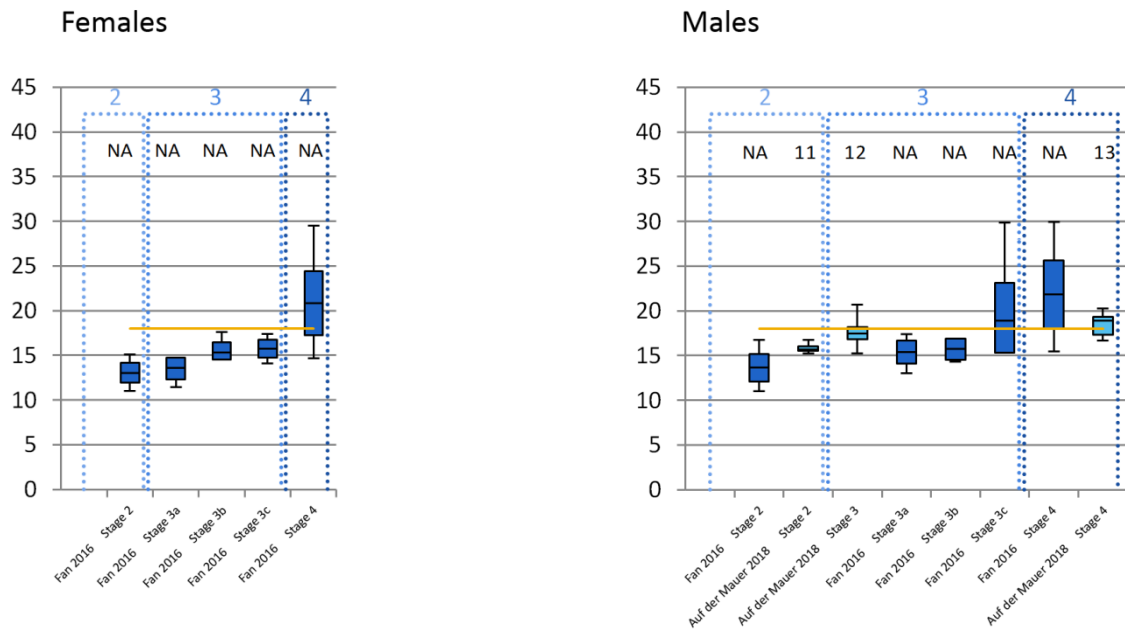


Fig. 5p Proximal fibula – Most elaborate staging technique.

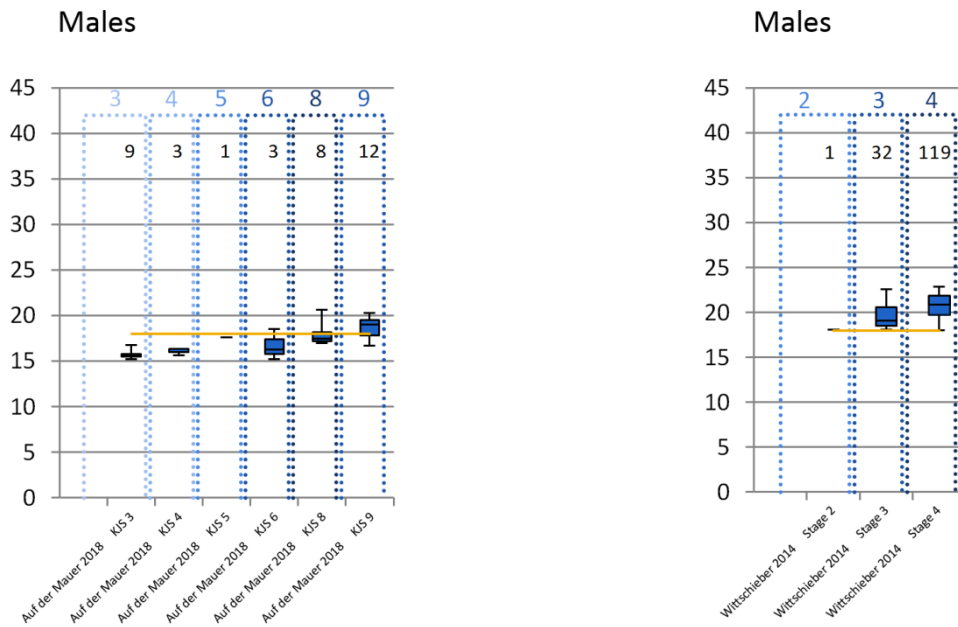


Fig. 5q Knee – Knee joint score (KJS = sum of Jopp stages of each knee bone).

Fig. 5r Iliac crest – Most elaborate staging technique.

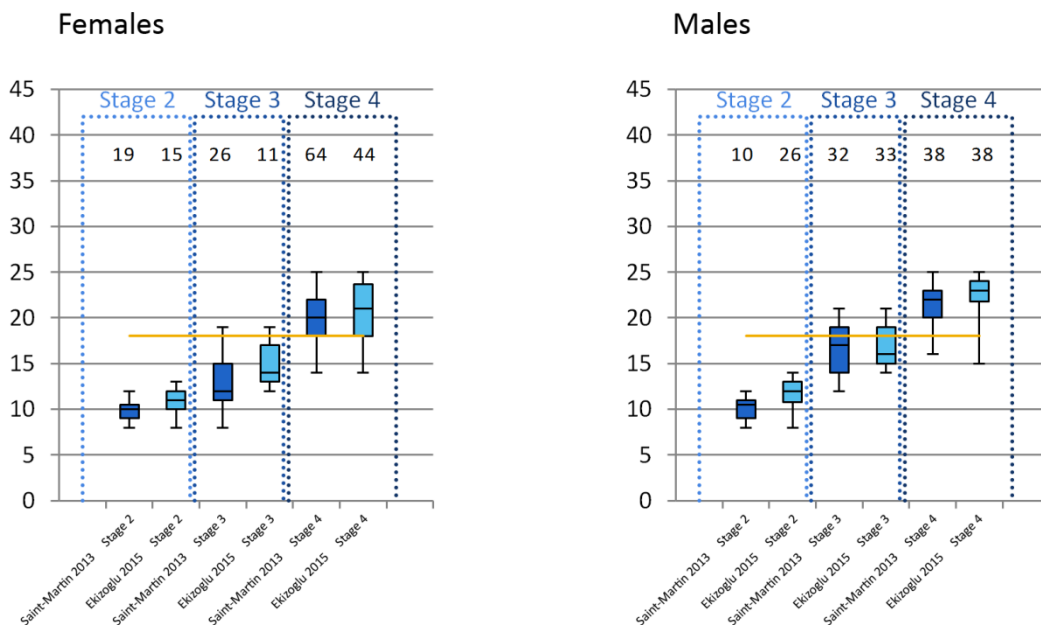


Fig. 5s Distal tibia – Most elaborate staging technique.

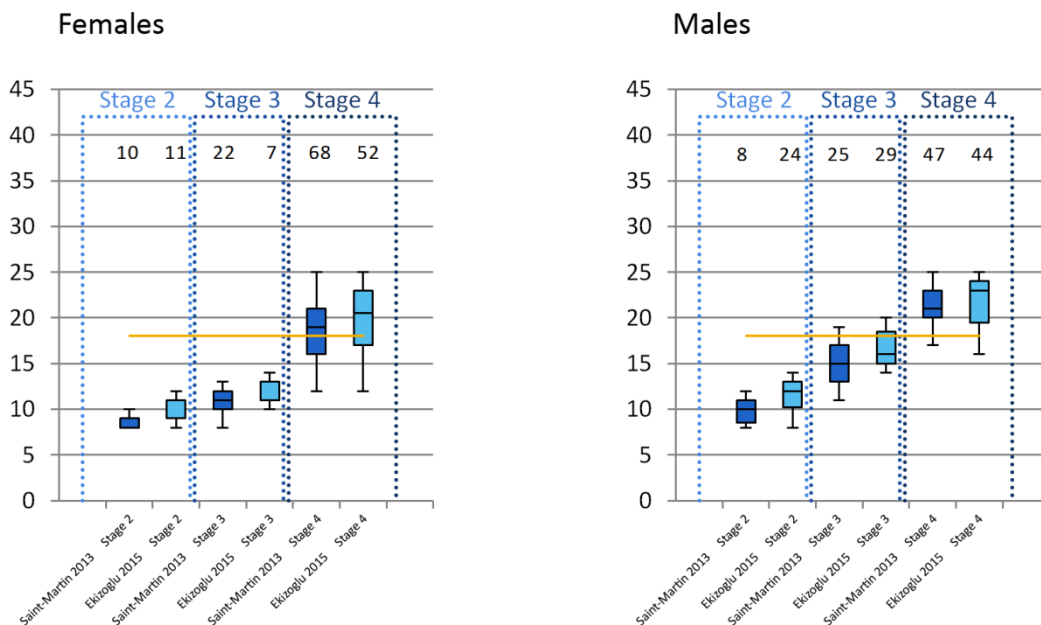


Fig. 5t Calcaneum – Most elaborate staging technique.

Reproducibility of staging

Table 8 displays the reproducibility statistics of different MRI approaches for age estimation.

**Table 8** Reproducibility statistics in the included studies. References are ordered in the same way as in Tables 1 and 5-7.

Anatomical structure	Reference	Year	Inter-observer variability					Intra-observer variability				
			Measure	Value	N participants	N structures	N observers	Measure	Value	N participants	N structures	N observers
Spheno-occipital synchondrosis	Ekizoglu	2016a	Cohen's kappa	0.907	1078	1078	2	Cohen's kappa	0.954	1078	1078	1
			Weighted kappa	0.981				Weighted kappa	0.990			
Molars (mineralization)	Baumann	2015	Cohen's kappa	0.51	18	262 molars	2	NA				
Molars (eruption)	Baumann	2015	Cohen's kappa	0.57	18	274 molars	2	NA				
Lower left third molar	Guo	2015	Kappa	0.83	60	60	2	Kappa coefficient	0.89	60	60	1
Third molars	De Tobel	2017	ICC	0.85-0.94	52	183 molars	2	ICC	0.94-0.98	52	Not specified	1
Third molars	De Tobel	2017	ICC	0.86-0.95	52	183 molars	2	ICC	0.94-0.98	52	Not specified	1
Third molars	De Tobel	2017	Weighted kappa	0.790	309	899	2	Weighted kappa	0.873	130	379	2
18	De Tobel	2017		0.803	309	899	2	18	0.857	130	379	2
28	De Tobel	2017		0.784	309	899	2	28	0.848	130	379	2
38	De Tobel	2017		0.764	309	899	2	38	0.890	130	379	2
48	De Tobel	2017		0.804	309	899	2	48	0.889	130	379	2
Clavicle	Hillewig	2013	Fleiss' kappa	0.76 left, 0.74 right	220	440	4	Cohen's kappa	0.75	20	Not specified	1
Clavicle	Tangmose	2014	Kappa (stages 1-3 collapsed)	-0.004-0.414; prone position 0.040-0.446	49-53	98-106; prone position 26-32	3	Kappa	0.669; prone position 0.788	53; prone position 32	106; prone position 64	1
Clavicle	Vieth	2014	NA					NA				
Clavicle	Schmidt	2017	Weighted kappa	0.987	80	160	2	Weighted kappa	0.991	80	160	1
Clavicle	De Tobel	2019c	Weighted kappa	0.64, 0.60, 0.61	NA	400, 471, 387	4	Weighted kappa	0.82	NA	186	1
			Kendall's coefficient of concordance	0.800	NA	400, 471, 387	4					
Manubrium	Martínez Vera	2017	NA					NA				
Proximal humerus	Ekizoglu	2018	Cohen's kappa	0.828	428	428	2	Cohen's kappa	0.898	NA	NA	NA
Left distal radius	Dvorak	2007	Correlation coefficient	0.91-0.92	496	496	3	NA				
Left distal radius	George	2012	Spearman	0.9	150	150	3	NA				
Left distal radius	Bolivar	2015	Kappa	0.23	60	60	3	Kappa	0.79	6	6	1
Left distal radius	Rashid	2015	NA					NA				
Left distal radius	Tscholl	2016	Kappa	0.928	487	487	2	NA				
Left distal radius	Abdelbary	2018	Weighted kappa	0.828	61	61	2	NA				
Left distal radius	Sarkodie	2018	Kappa	0.95	286	286	3	NA				
Left distal radius	Schmidt	2015	Kappa	0.88	30	30	2	Kappa	0.94	30	30	1
Left distal radius	Serin	2016	Cohen's kappa	0.81	263	263	2	Cohen's kappa	0.93	263	263	1
Left distal ulna	Serin	2016		0.88	263	263	2		0.94	263	263	1
Left proximal first metacarpus	Serin	2016		0.84	263	263	2		0.95	263	263	1
Left distal radius	Timme	2017	Cohen's kappa	0.974	100	100	2	Cohen's kappa	0.988	100	100	2
Left distal radius SE	De Tobel	2019b	Weighted kappa	0.792	361	361	2	Weighted kappa	0.856	98	98	1
Left distal radius VIBE			Weighted kappa	0.712	359	359	2	Weighted kappa	0.843	98	98	1
Left hand/wrist	Tomei	2014	Pearson	0.95 F, 0.97 M	78 F, 101 M	179 x 9 bones	2	NA				
Left hand/wrist	Serinelli	2015	Pearson	0.97 F, 0.98 M	151	151 x 9 bones	2	Bland-Altman plots	NA	151	151 x 9 bones	1
Left hand/wrist	Terada	2013	Pearson	0.922-0.926	83	83 x 13 bones	2	Pearson	0.958	83	83 x 13 bones	1
Left hand/wrist	Terada	2014	Pearson	0.880-0.935	88	88 x 13 bones	3	Pearson	0.918	88	88 x 13 bones	1
Left hand/wrist	Terada	2016	Pearson	0.956-0.964	59	59 x 13 bones	2	Pearson	0.959	59	59 x 13 bones	1
Left hand/wrist	Urschler	2016	Weighted kappa	GP 0.74; TW2 0.51	18	GP 18; TW2 18 x 13 bones	2	NA				
Left hand/wrist	Hojreh	2018	ICC	0.95 F; 0.97 M	33; 17	22; 15	2	NA				
Left hand/wrist	Urschler	2015	NA					NA				

Table 8 (continued) Reproducibility statistics in the included studies.

Anatomical structure	Reference	Year	Inter-observer variability				Intra-observer variability					
			Measure	Value	N participants	N structures	N observers	Measure	Value	N participants	N structures	N observers
Iliac crest	Wittschieber	2014	NA					NA				
Proximal femur	Vo	2015	ICC	0.694	43	86	3	ICC	0.788	43	86	1
Sacrum	Bollow	1997	NA					NA				
Sacrum	Bollow	1997	NA					NA				
Patellofemoral joint	Kim	2014	NA					NA				
Distal femur	Saint-Martin	2015	Cohen's kappa	0.86	214	214	2	Cohen's kappa	0.86	214	214	1
Distal femur	Dedouit	2012	Cohen's kappa	0.86	290	290	2	Cohen's kappa	0.96	290	290	1
Proximal tibia	Dedouit	2012	Cohen's kappa	0.63	290	290	2	Cohen's kappa	0.96	290	290	1
Distal femur	Ekizoglu	2016b	Cohen's kappa	0.836	503	503	2	Cohen's kappa	0.919	503	503	1
			Weighted kappa	0.954				Weighted kappa	0.978			
Proximal tibia	Ekizoglu	2016b	Cohen's kappa	0.885	503	503	2	Cohen's kappa	0.961	503	503	1
			Weighted kappa	0.979				Weighted kappa	0.993			
Knee	Harcke	1992	NA					NA				
Knee	Laor	2002	NA					NA				
Proximal tibia	Jopp	2010	NA					NA				
Distal femur	Krämer	2014a	Kappa	0.85	30	30	2	Kappa	0.94	30	30	1
Proximal tibia	Krämer	2014b	Kappa	0.85	30	30	2	Kappa	0.88	30	30	1
Distal femur	Fan	2016	ICC	0.946	322	322	2	ICC	0.967	322	322	1
Proximal tibia	Fan	2016	ICC	0.978	322	322	2	ICC	1.000	322	322	1
Proximal fibula	Fan	2016	ICC	0.931	322	322	2	ICC	0.965	322	322	1
Distal femur	Ottow	2017	Kappa	0.941	115	115	2	Kappa	0.961	115	115	1
Proximal tibia	Ottow	2017	Kappa	0.951	115	115	2	Kappa	0.971	115	115	1
Knee	Auf der Mauer	2018	Fleis' kappa	0.840	36	104	3	NA				
Distal femur	Auf der Mauer	2018	Fleis' kappa	0.799	36	104	3	NA				
Proximal tibia	Auf der Mauer	2018	Fleis' kappa	0.886	36	104	3	NA				
Proximal fibula	Auf der Mauer	2018	Fleis' kappa	0.833	36	104	3	NA				
Distal femur	Vieth	2018	Cohen's kappa	0.913	100	100	2	Cohen's kappa	0.914	100	100	1
Proximal tibia	Vieth	2018	Cohen's kappa	0.847	100	100	2	Cohen's kappa	0.893	100	100	1
Knee	Pennock	2018	ICC	0.957	323	323	2	ICC	0.992	323	323	NA
Knee	Craig	2004	NA					NA				
Knee	Kercher	2009	NA					NA				
Distal tibia	Saint-Martin	2013	Cohen's kappa	0.84	180	180	2	Cohen's kappa	0.97	180	180	1
Calcaneum	Saint-Martin	2013	Cohen's kappa	0.90	180	180	2	Cohen's kappa	0.97	180	180	1
Distal tibia	Saint-Martin	2014	NA					NA				
Distal tibia	Ekizoglu	2015	Cohen's kappa	0.834	167	167	2	Cohen's kappa	0.883	167	167	2
Calcaneum	Ekizoglu	2015	Cohen's kappa	0.802	167	167	2	Cohen's kappa	0.811	167	167	2
MFA	Stern	2017	NA					NA				

F = females; GP = Greulich-Pyle atlas technique; ICC = intra-class correlation coefficient; M = males; NA = not applicable or not reported; SE = spin echo MR-sequence; TW2 = Tanner-Whitehouse-2 atlas technique; VIBE = volumetric interpolated breath-hold examination MR-sequence

When data from different observers was available, those were separately included in Fig. 5. Note that the inter-observer differences were mostly subtle, but might have severe consequences around the age of 18. For instance, Fig. 5f shows that females categorized by observer 1 into the age standard of 17 years old were relatively younger than for observer 2 [30]. Few studies included cross-tabulations of different observers' results [27-29], which demonstrate that discrepancies are mostly within neighboring stages.

### Supplementary text references

1. Harcke HT, Synder M, Caro PA, Bowen JR (1992) Growth plate of the normal knee: evaluation with MR imaging. *Radiology* 183:119-123.
2. Laor T, Chun GF, Dardzinski BJ, Bean JA, Witte DP (2002) Posterior distal femoral and proximal tibial metaphyseal stripes at MR imaging in children and young adults. *Radiology* 224:669-674.
3. Bollow M, Braun J, Kannenberg J, Biedermann T, Schauer-Petrowskaja C, Paris S, Mutze S, Hamm B (1997) Normal morphology of sacroiliac joints in children: magnetic resonance studies related to age and sex. *Skeletal Radiol* 26:697-704.
4. Craig JG, Cody DD, Van Holsbeeck M (2004) The distal femoral and proximal tibial growth plates: MR imaging, three-dimensional modeling and estimation of area and volume. *Skeletal Radiol* 33:337-344.
5. Bray TJ, Vendhan K, Roberts J, Atkinson D, Punwani S, Sen D, Ioannou Y, Hall-Craggs MA (2016) Association of the apparent diffusion coefficient with maturity in adolescent sacroiliac joints. *J Magn Reson Imaging* 44:556-564.
6. George J, Nagendran J, Azmi K (2012) Comparison study of growth plate fusion using MRI versus plain radiographs as used in age determination for exclusion of overaged football players. *Br J Sports Med* 46:273-278.
7. Kercher J, Xerogeanes J, Tannenbaum A, Al-Hakim R, Black JC, Zhao J (2009) Anterior cruciate ligament reconstruction in the skeletally immature: an anatomical study utilizing 3-dimensional magnetic resonance imaging reconstructions. *J Pediatr Orthop* 29:124-129.
8. Kim HK, Shiraj S, Anton C, Horn PS (2014) The patellofemoral joint: do age and gender affect skeletal maturation of the osseous morphology in children? *Pediatr Radiol* 44:141-148.
9. Martinez Vera NP, Holler J, Widek T, Neumayer B, Ehammer T, Urschler M (2017) Forensic age estimation by morphometric analysis of the manubrium from 3D MR images. *Forensic Sci Int* 277:21-29.
10. Pennock AT, Bomar JD, Manning JD (2018) The Creation and Validation of a Knee Bone Age Atlas Utilizing MRI. *J Bone Joint Surg Am* 100:e20.
11. Saint-Martin P, Rerolle C, Pucheux J, Dedouit F, Telmon N (2015) Contribution of distal femur MRI to the determination of the 18-year limit in forensic age estimation. *Int J Legal Med* 129:619-620.
12. Sarkodie BD, Botwe BO, Pambo P, Brakohiapa EK, Mayeden RN (2018) MRI age verification of U-17 footballers: The Ghana study. *J Forensic Radiol Imaging* 12:21-24.
13. Štern D, Kainz P, Payer C, Urschler M (2017) Multi-Factorial Age Estimation from Skeletal and Dental MRI Volumes. In: *International Workshop on Machine Learning in Medical Imaging*. Springer, Quebec City, Canada, pp 61-69.

14. Tangmose S, Jensen KE, Villa C, Lynnerup N (2014) Forensic age estimation from the clavicle using 1.0T MRI-Preliminary results. *Forensic Sci Int* 234:7-12.
15. Terada Y, Kono S, Tamada D, Uchiumi T, Kose K, Miyagi R, Yamabe E, Yoshioka H (2013) Skeletal age assessment in children using an open compact MRI system. *Magn Reson Med* 69:1697-1702.
16. Terada Y, Kono S, Uchiumi T, Kose K, Miyagi R, Yamabe E, Fujinaga Y, Yoshioka H (2014) Improved reliability in skeletal age assessment using a pediatric hand MR scanner with a 0.3T permanent magnet. *Magn Reson Med* 13:215-219.
17. Terada Y, Tamada D, Kose K, Nozaki T, Kaneko Y, Miyagi R, Yoshioka H (2016) Acceleration of skeletal age MR examination using compressed sensing. *J Magn Reson Imaging* 44:204-211.
18. Tomei E, Sartori A, Nissman D, Al Ansari N, Battisti S, Rubini A, Stagnitti A, Martino M, Marini M, Barbato E, Semelka RC (2014) Value of MRI of the hand and the wrist in evaluation of bone age: Preliminary results. *J Magn Reson Imaging* 39:1198-1205.
19. Urschler M, Krauskopf A, Widek T, Sorantin E, Ehammer T, Borkenstein M, Yen K, Scheurer E (2016) Applicability of Greulich-Pyle and Tanner-Whitehouse grading methods to MRI when assessing hand bone age in forensic age estimation: A pilot study. *Forensic Sci Int* 266:281-288.
20. Vo A, Beaulé PE, Sampaio ML, Rotaru C, Rakhra KS (2015) The femoral head-neck contour varies as a function of physal development. *Bone Joint Res* 4:17-22.
21. Baumann P, Widek T, Merkens H, Boldt J, Petrovic A, Urschler M, Kirnbauer B, Jakse N, Scheurer E (2015) Dental age estimation of living persons: Comparison of MRI with OPG. *Forensic Sci Int* 253:76-80.
22. De Tobel J, Hillewig E, Verstraete K (2017) Forensic age estimation based on magnetic resonance imaging of third molars: converting 2D staging into 3D staging. *Ann Hum Biol* 44:121-129.
23. Jopp E, Schröder I, Maas R, Adam G, Püschel K (2010) Proximal tibial epiphysis in magnetic resonance imaging. *Rechtsmedizin* 20:464-468.
24. Tscholl PM, Junge A, Dvorak J, Zubler V (2016) MRI of the wrist is not recommended for age determination in female football players of U-16/U-17 competitions. *Scand J Med Sci Sports* 26:324-328.
25. Urschler M, Grassegger S, Stern D (2015) What automated age estimation of hand and wrist MRI data tells us about skeletal maturation in male adolescents. *Ann Hum Biol* 42:358-367.
26. Auf der Mauer M, Saring D, Stanczus B, Herrmann J, Groth M, Jopp-van Well E (2018) A 2-year follow-up MRI study for the evaluation of an age estimation method based on knee bone development. *Int J Legal Med* 133:205-215.
27. De Tobel J, Hillewig E, de Haas MB, Van Eeckhout B, Fieuws S, Thevissen P, Verstraete K (2019) Forensic age estimation based on T1 SE and VIBE wrist MRI: do a one-fits-all staging technique and age estimation model apply? *Eur Radiol* 26:2924-2935.
28. De Tobel J, Hillewig E, van Wijk M, Fieuws S, de Haas MB, van Rijn RR, Thevissen PW, Verstraete KL (2019) Staging clavicular development on magnetic resonance imaging: pitfalls and recommendations for age estimation. *J Magn Reson Imaging*:[Epub ahead of print].
29. De Tobel J, Phlypo I, Fieuws S, Politis C, Verstraete KL, Thevissen PW (2017) Forensic age estimation based on development of third molars: a staging technique for magnetic resonance imaging. *J Forensic Odontostomatol* 35:117-140.
30. Hojreh A, Gamper J, Schmook MT, Weber M, Prayer D, Herold CJ, Noebauer-Huhmann IM (2018) Hand MRI and the Greulich-Pyle atlas in skeletal age estimation in adolescents. *Skeletal Radiol* 47:963-971.
31. Hillewig E, De Tobel J, Cuche O, Vandemaele P, Piette M, Verstraete K (2011) Magnetic resonance imaging of the medial extremity of the clavicle in forensic bone age determination: a new four-minute approach. *Eur Radiol* 21:757-767.
32. De Tobel J, Hillewig E, Bogaert S, Deblaere K, Verstraete K (2017) Magnetic resonance imaging of third molars: developing a protocol suitable for forensic age estimation. *Ann Hum Biol* 44:130-139.
33. Dedouit F, Auriol J, Rousseau H, Rouge D, Crubezy E, Telmon N (2012) Age assessment by magnetic resonance imaging of the knee: a preliminary study. *Forensic Sci Int* 217:232 e231-237.
34. Ekizoglu O, Hocaoglu E, Inci E, Can IO, Aksoy S, Kazimoglu C (2016) Forensic age estimation via 3-T magnetic resonance imaging of ossification of the proximal tibial and distal femoral epiphyses: Use of a T2-weighted fast spin-echo technique. *Forensic Sci Int* 260:102.e101-107.
35. Vieth V, Schulz R, Heindel W, Pfeiffer H, Buerke B, Schmeling A, Ottow C (2018) Forensic age assessment by 3.0T MRI of the knee: proposal of a new MRI classification of ossification stages. *Eur Radiol* 28:3255-3262.

36. Schmidt S, Vieth V, Timme M, Dvorak J, Schmeling A (2015) Examination of ossification of the distal radial epiphysis using magnetic resonance imaging. New insights for age estimation in young footballers in FIFA tournaments. *Sci Justice* 55:139-144.
37. Timme M, Ottow C, Schulz R, Pfeiffer H, Heindel W, Vieth V, Schmeling A, Schmidt S (2017) Magnetic resonance imaging of the distal radial epiphysis: a new criterion of maturity for determining whether the age of 18 has been completed? *Int J Legal Med* 131:579-584.
38. Tomei E, Semelka RC, Nissman D (2013) Text-atlas of skeletal age determination: MRI of the hand and wrist in children. John Wiley & Sons.
39. Tanner JM, Whitehouse RH, Cameron N, Marshall WA, Healy MJR, Goldstein H (1983) Assessment of skeletal maturity and prediction of adult height (TW2 method). Academic Press Limited, London.
40. Greulich W, Pyle SI (1959) Radiographic atlas of skeletal development of the hand and wrist. Stanford University Press, Stanford, CA.
41. Ekizoglu O, Inci E, Ors S, Kacmaz IE, Basa CD, Can IO, Kranioti EF (2018) Applicability of T1-weighted MRI in the assessment of forensic age based on the epiphyseal closure of the humeral head. *Int J Legal Med* 133:241-248.
42. Guo Y, Olze A, Ottow C, Schmidt S, Schulz R, Heindel W, Pfeiffer H, Vieth V, Schmeling A (2015) Dental age estimation in living individuals using 3.0 T MRI of lower third molars. *Int J Legal Med* 129:1265-1270.
43. Dvorak J, George J, Junge A, Hodler J (2007) Age determination by magnetic resonance imaging of the wrist in adolescent male football players. *Br J Sports Med* 41:45-52.
44. Ottow C, Schulz R, Pfeiffer H, Heindel W, Schmeling A, Vieth V (2017) Forensic age estimation by magnetic resonance imaging of the knee: the definite relevance in bony fusion of the distal femoral- and the proximal tibial epiphyses using closest-to-bone T1 TSE sequence. *Eur Radiol* 27:5041-5048.
45. Vieth V, Schulz R, Brinkmeier P, Dvorak J, Schmeling A (2014) Age estimation in U-20 football players using 3.0 tesla MRI of the clavicle. *Forensic Sci Int* 241c:118-122.
46. Wittschieber D, Vieth V, Timme M, Dvorak J, Schmeling A (2014) Magnetic resonance imaging of the iliac crest: age estimation in under-20 soccer players. *Forensic Sci Med Pathol* 10:198-202.
47. Bolívar J, Sandoval Ó, Osorio J, Dib G, Gallo J (2015) Relationship of chronological age and sexual maturity with skeletal maturity by magnetic resonance imaging of the distal radial epiphysis in adolescent football players. *Apunts Medicina de l'Esport* 50:129-137.
48. Rashid NR, Aliasghar A, Shaker QM (2015) Magnetic resonance imaging of the left wrist: assessment of the bone age in a sample of healthy Iraqi adolescent males. *J Fac Med Baghdad* 57:22-26.
49. Abdelbary MH, Abdelkawi MM, Nasr MA (2018) Age determination by MR imaging of the wrist in Egyptian male football players. How far is it reliable? *Egyptian Journal of Radiology and Nuclear Medicine* 49:146-151.
50. Serinelli S, Panebianco V, Martino M, Battisti S, Rodacki K, Marinelli E, Zaccagna F, Semelka RC, Tomei E (2015) Accuracy of MRI skeletal age estimation for subjects 12-19. Potential use for subjects of unknown age. *Int J Legal Med* 129:609-617.
51. Ekizoglu O, Hocaoglu E, Can IO, Inci E, Aksoy S, Sayin I (2016) Spheno-occipital synchondrosis fusion degree as a method to estimate age: A preliminary, magnetic resonance imaging study. *Aust J Forensic Sci* 48:159-170.
52. Hillewig E, Degroote J, Van der Paelt T, Visscher A, Vandemaele P, Lutin B, D'Hooghe L, Vandriessche V, Piette M, Verstraete K (2013) Magnetic resonance imaging of the sternal extremity of the clavicle in forensic age estimation: towards more sound age estimates. *Int J Legal Med* 127:677-689.
53. Saint-Martin P, Rerolle C, Dedouit F, Bouilleau L, Rousseau H, Rouge D, Telmon N (2013) Age estimation by magnetic resonance imaging of the distal tibial epiphysis and the calcaneum. *Int J Legal Med* 127:1023-1030.